

TOPICAL REVIEW • OPEN ACCESS

Recent progress of neuromorphic sensory and optoelectronic systems

To cite this article: San Nam *et al* 2025 *Int. J. Extrem. Manuf.* **7** 042006

View the [article online](#) for updates and enhancements.

You may also like

- [Performance-control-orientated hybrid metal additive manufacturing technologies: state of the art, challenges, and future trends](#)
Jiming Lv, Yuchen Liang, Xiang Xu et al.
- [Review on laser directed energy deposited aluminum alloys](#)
Tian-Shu Liu, Peng Chen, Feng Qiu et al.
- [Nontraditional energy-assisted mechanical machining of difficult-to-cut materials and components in aerospace community: a comparative analysis](#)
Guolong Zhao, Biao Zhao, Wenfeng Ding et al.

Topical Review

Recent progress of neuromorphic sensory and optoelectronic systems

San Nam^{1,§}, Donghyun Kang^{1,§}, Jeong-Wan Jo², Dong-Won Kang³, Sung Kyu Park^{3,*} and Yong-Hoon Kim^{1,*} 

¹ School of Advanced Materials Science and Engineering, Sungkyunkwan University (SKKU), Suwon 16419, Republic of Korea

² Electrical Engineering Division, Department of Engineering, University of Cambridge, CB2 1TN Cambridge, United Kingdom

³ Displays and Devices Research Lab, Department of Intelligent Semiconductor Engineering, Chung-Ang University, Seoul 06974, Republic of Korea

E-mail: skpark@cau.ac.kr and yhkim76@skku.edu

Received 1 October 2024, revised 22 December 2024

Accepted for publication 26 February 2025

Published 3 April 2025



CrossMark

Abstract

With the rise of artificial intelligence (AI), neuromorphic sensory systems that emulate the five basic human sensations including tactility, audition, olfaction, gustation, and vision have attracted significant attention. In particular, research on integrating sensors with artificial synapses is being carried out extensively. These studies offer valuable opportunities for making another breakthrough in AI technology, including autonomous systems, real-time monitoring systems, and human-machine interactions. In this review, we introduce promising reports of neuromorphic sensory systems. Specifically, the core sensing material, device architecture, fabrication process, and applications of the proposed systems are presented in detail. Finally, the unsolved challenges and the prospects of neuromorphic sensory systems are discussed.

Keywords: artificial intelligence, neuromorphic sensory system, human sensation, sensor

1. Introduction

In the past decade, the age of artificial intelligence (AI) has arrived at a point where the impact of AI on human society has never been more prominent. Although AI is advancing at an unprecedented rate, there are still some challenges to be overcome, since the final goal of AI technology is

the creation of autonomous AI system implemented into an actual hardware such as humanoid robots. In this regard, emulating human sensory perception is crucial for humanoid robots to collect information from the various environmental conditions^[1,2]. However, human sensory perception is a complex phenomenon which is challenging to mimic. When a human encounters certain stimuli through sensory receptors in the organs, the concept of sensation is initiated^[3]. Then, the sensation is transmitted to the brain, where it interprets the sensory information and orders a suitable action. This complicated process is completed within a millisecond scale, indicating that the artificial sensory systems should not only detect diverse external stimuli, but also be able to convert the stimuli into signals and transmit them, thereby triggering subsequent responses^[4].

To mimic the biological sensory perception, artificial sensory systems in research are endeavoring to converge a sensor

§ These authors contributed equally to this work and should be considered co-first author.

* Authors to whom any correspondence should be addressed.



Original content from this work may be used under the terms of the [Creative Commons Attribution 4.0 licence](https://creativecommons.org/licenses/by/4.0/). Any further distribution of this work must maintain attribution to the author(s) and the title of the work, journal citation and DOI.

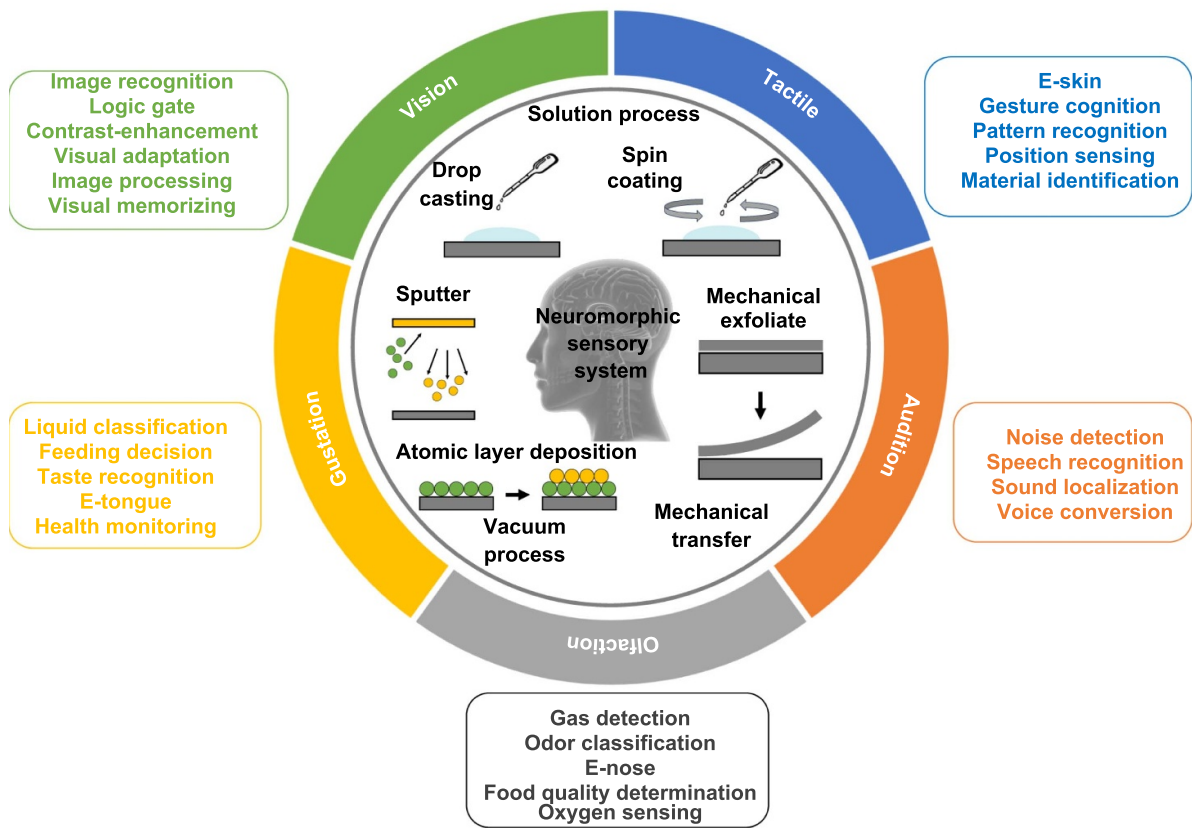


Figure 1. Schematic diagrams of various fabrication methods and applications of neuromorphic sensory systems. Five basic biological sensations are represented through artificial sensors fabricated via solution process, vacuum process, and mechanical transfer process. The applications of neuromorphic sensory systems include detection, recognition, and classification of diverse signals, electronic organs, and adaptive monitoring systems.

with an artificial synapse^[5]. Here, the sensor serves the role as a sensory organ, while the synaptic device acts as a biological synapse that transmits and learns the sensory information. For the sensors, various materials with different types of device configurations have been utilized for the replication of biological sensory organs. Few requirements must be met to ensure high-performance sensors. Since there is a limitation in the performance of real human sensory organs, it is crucial to maximize the sensitivity and lower the detection limit in order to enhance the performance of the sensory system. Securing the biocompatibility and ambient stability of sensors is also significant to realize the implantation of sensors in humans or humanoids. In case of artificial synapses, memristors, memtransistors, organic electrochemical transistors (OECTs), and other synaptic devices are commonly utilized^[6–15]. These devices are capable of emulating a variety of synaptic functions such as the short-term plasticity (STP), long-term potentiation (LTP), long-term depression (LTD), paired pulse facilitation (PPF), and spike timing dependent plasticity (STDP), which are the key mechanisms in realizing neuromorphic sensors. Moreover, the synaptic functions of these devices can be coupled with artificial neural networks (ANNs) and machine learning (ML) algorithms, broadening the applicability of the neuromorphic sensory system^[16,17].

This review aims to provide an overview of integrated neuromorphic sensory systems and their applications as depicted in Figure 1. The neuromorphic sensory systems discussed in this review include tactile, auditory, olfactory, gustatory, and vision systems which constitute the biological sensory system altogether. First, we clarify the importance of linking sensory information with synaptic functions. Afterward, we will discuss about the neuromorphic sensory systems classified according to various significant aspects. In each section, we also provide the current limitations of the reported systems and comparative analyses regarding each classification criteria. Section 2 will be focused on the artificial tactile sensors classified according to the core sensing materials which are divided into organic and inorganic materials. In Section 3, auditory sensory systems will be introduced based on various fabrication methods. These methods include solution-based fabrication (evaporation-based technique, and direct patterning techniques) and the combination of vacuum processes with other methods. Section 4 offers an elaborate explanation of artificial olfactory and gustatory systems. Here, the olfactory systems and gustatory systems were organized by the structure of the device and the form of integration, respectively. Specifically, the heterogeneous integration refers to the form in which a sensor is connected with an artificial synapse. In other words, this system integrates a sensor device

that serves as a sensory neuron and a distinct synaptic part that processes the sensory information. On the other hand, monolithically integrated system comprises of a single device that can emulate a sensory neuron and a synapse simultaneously. Next, advanced neuromorphic vision sensors and optoelectronic devices are extensively explored in Section 5. In this section, optoelectronic visual devices are categorized by the materials including low-dimensional, oxide, ferroelectric, organic, and perovskite materials. Moreover, a variety of optoelectronic applications such as visual adaptation, image processing, and ANN-based tasks are comprehensively reviewed. Finally, we will briefly summarize the artificial sensory systems. Most importantly, we offer a detailed discussion of the current challenges regarding the mass production and commercialization of neuromorphic sensory systems which are deemed as critical bottlenecks in this area, along with specific future research directions that may provide useful insights. We also stress the significance of interdisciplinary collaboration, suggesting specific contributions that each discipline is desired to make. Overall, we believe this review paper can offer comprehensive information about state-of-the-art neuromorphic sensory systems, reducing the gap between academia and industry, and also provide a clear guidance for the development of highly sophisticated neuromorphic systems.

2. Neuromorphic tactile sensors

Tactile sensors emulate the combined efforts of various touch receptors, through which tactile sensation is created. For instance, mechanoreceptors react to physical pressure and tactile stimuli, thermoreceptors to temperature, and nociceptors to pain. Previously, studies of tactile sensors have been contingent on sensing performance itself, with limited applicability. In recent years, however, diverse applications including robotic systems, prosthetics, human-machine interface (HMI), and biomedical applications have gained considerable attention. Generally, these applications require the implementation of tactile sensors, along with the combination with the artificial nervous system. This hybridization can directly emulate the biological tactile perception, facilitating the tactile information processing of the systems. Therefore, research on integrating tactile sensors with neuromorphic systems is highly desirable.

Neuromorphic tactile systems in research show a variety of applications utilizing a broad range of materials, system components, and fabrication methods. The core material of tactile systems hugely influences the manufacturing process and the performance of the system. The potential applications are affected as well. Thus, we focus on the recent reports on different types of integrated neuromorphic tactile systems categorized by organic-based and inorganic-based tactile systems (Table 1).

2.1. Organic-based tactile systems

Organic materials are one of the most widely used materials for neuromorphic sensory devices. They are especially suitable for flexible and wearable tactile sensory systems such as e-skin, due to their large-scale solution processability, flexibility, direct patterning capability, and biocompatibility^[28,29]. Moreover, most organic materials are compatible with each other, enabling a huge variety of material combinations for converged artificial sensory systems. For example, many functional polymers have been successfully implemented into numerous tactile systems, since they can be easily integrated into electronic systems. Among various polymer materials, poly(vinylidene fluoride-trifluoroethylene) P(VDF-TrFE) is widely used for tactile sensors owing to its versatility. It can be both utilized as a ferroelectric material for ferroelectric field-effect transistors (FETs), or as a piezoelectric material for tactile sensors^[30]. Huynh et al. featured artificial adaptive mechanoreceptors using a P(VDF-TrFE)-based piezoelectric pressure sensor^[18]. Here, the piezoelectric pressure sensors were integrated with synaptic electrolyte-gated FETs (EGFETs) to emulate the fast-adaptive (FA) receptors and slow-adaptive (SA) receptors. For the operating mechanism, piezoelectric and piezoelectric-ionic coupling potentials were generated upon the application of external pressure stimuli, triggering a synaptic effect from the EGFETs. Poly(dimethylsiloxane) (PDMS), poly(tetrafluoroethylene) (PTFE), and polyimide are other types of polymers specialized for tactile sensors that are based on triboelectricity^[21]. Kim et al. reported an integrated tactile neuromorphic system which consists of a PDMS-based triboelectric sensor and a ferroelectric synapse^[31]. The self-powered neuromorphic tactile system with a PTFE-based triboelectric nanogenerator (TENG) and a bi-stable resistor (biristor) was also presented, showcasing the high applicability of polymers for neuromorphic sensory systems^[21].

Ionic-gel is another class of organic material which has recently gained considerable attention for constituting diverse neuromorphic devices owing to their biocompatibility, mechanical flexibility, high capacitance, low-voltage operation, and biomimetic electrical properties^[32,33]. Further, the versatility of ionic gels allows them to be used as a tactile sensor itself or a gate dielectric material for synaptic devices. Niu et al. presented an electronic skin (e-skin) inspired by the human full-skin bionic structure (Figures 2(a) and (b))^[20]. The proposed system can be described as an assembly of triboelectric e-skin stacked with a piezocapacitive ionotronic e-skin. Specifically, the piezocapacitive effect of layered micro-cone structure poly(vinylidene fluoride-co-hexafluoropropylene)/1-ethyl-methylimidazolium bis(trifluoromethylsulfonyl)imide ([EMIM][TFSI]) ionic gel was used to imitate the skin dermis. This layer was connected with triboelectric layer which emulates the human vellus hair and epidermis. Together, the tactile perception of external stimuli and the sign language cognition

Table 1. Summary of neuromorphic tactile and auditory systems.

Year	Material	Manufacturing	Structure	Applications	Recognition accuracy	References
2022	P(VDF-TrFe) Ionic gel	Solution process	Two terminal structure (sensor) Three terminal structure (synapse)	Adaptive mechanoreceptor	N/A	[18]
2024	MWCNT	Solution process	Multiterminal structure	Letter, location, slide direction recognition	97.1% 92.9%	[19]
2022	PVDF-HFP ionic gel	Solution process	Two terminal structure	Gesture cognition Robot interaction	98.34%	[20]
2022	PTFE	Photolithography	Two terminal structure (sensor) Two terminal structure (neuron)	SNN MNIST digit pattern classification	85.8%	[21]
2020	MXene	Solution process	Two terminal structure (sensor) Two terminal structure (synapse)	Letter recognition Word Classification	N/A	[22]
2023	Ionic gel	Solution process	Three terminal structure	Robotic hand system	N/A	[23]
2020	2D materials	Vacuum process	Three terminal structure	Acoustic pattern recognition (ANN)	93.8%	[24]
2020	Metal oxide	Solution process	Three terminal structure	Acoustic response system	N/A	[25]
2022	MXene	Solution process	Two terminal structure	Real-time voice signal classification	96.4% 95%	[26]
2023	Polymer	Vacuum process	Two terminal structure (sensor) Two terminal structure (synapse)	SNN Pitch classification	N/A	[27]

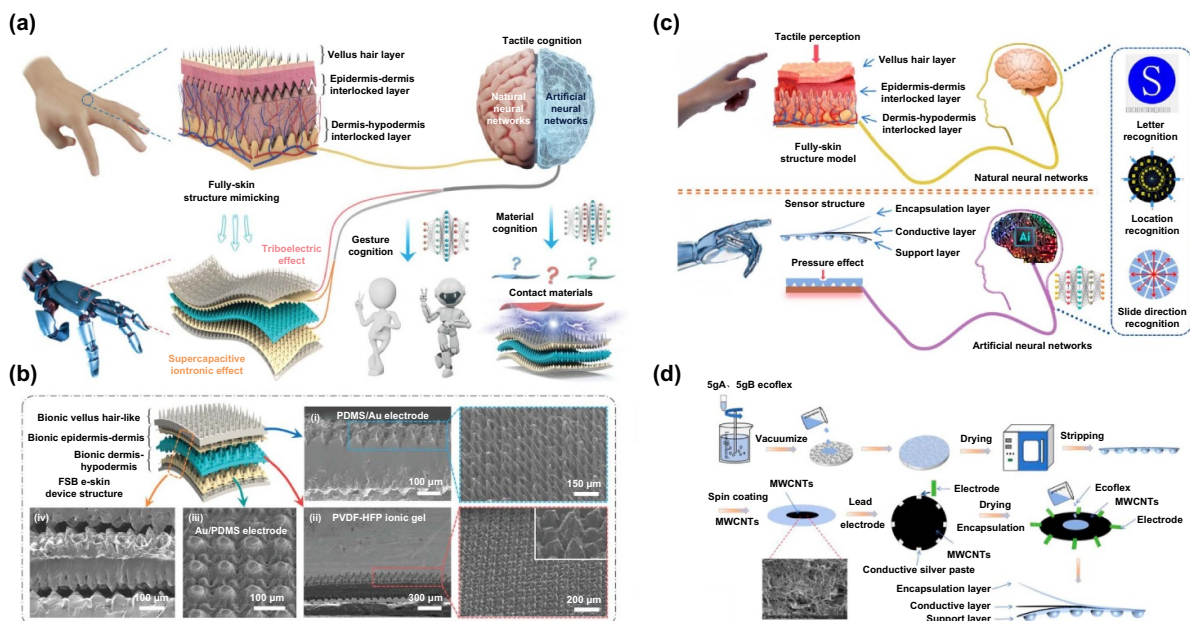


Figure 2. Neuromorphic tactile systems based on various organic and inorganic materials. (a) Conceptual diagram of the constructed e-skin. Triboelectric and supercapacitive iontronic effects were used to emulate the sensing process of human skin. Through the constructed e-skin, Gesture and material cognition tasks were carried out. (b) Specific structure of the proposed e-skin and the scanning electron microscope (SEM) images of the electrodes and ionic gel obtained from cross-sectional and tilted views. (a) and (b)^[20] John Wiley & Sons. © 2022 Wiley-VCH GmbH. (c) Illustration of the device structure and concept coupled with the human skin structure and tactile perception process, respectively. Here, the sensory system was utilized for letter, location, slide direction recognition tasks. (d) Stepwise fabrication of MWCNT-based tactile sensor by solution-process. (c) and (d) Reprinted (adapted) with permission from^[19]. Copyright (2024) American Chemical Society.

with robotic interactions were achieved, thereby realizing the recognition of materials and spatial locations. Organic dielectric elastomers including nitrile-butadiene rubber (NBR) and poly(styrene-ethylene-butylene-styrene) (SEBS) have been gaining considerable interest for flexible organic synaptic transistors. While ionic gel dielectrics can encounter a decrease in permittivity under high-frequency device operation^[34], dielectric elastomers can maintain their permittivity within wide frequency ranges^[35]. Also, their flexibility allows high applicability for e-skin systems. Wang et al. reported a monolithically integrated low-voltage e-skin system that emulates the biological sensorimotor loop^[36]. Here, an organic synaptic transistor with trilayer dielectric including NBR, SEBS, and hydrophobic octadecyltrimethoxysilane were utilized. The triple stack of dielectric layer boosted the carrier mobility of the synaptic transistor by 50 times, compared to single-layer NBR devices. Further, the breakdown voltage of the transistor was increased, with fewer defects observed in the dielectric layer. These enhanced electrical performances enabled low-voltage operation of the e-skin system, with low power consumption and a driving voltage of ± 0.5 V under 100% strain. Organic semiconductors such as pentacene and p-type {poly[2,5-bis(2-decyltetradecyl)-3-{5(thieno[3,2-b]thiophen-2-yl)thiophen-2-yl}-6-(thiophen-2-yl)pyrrolo[3,4-c]pyrrole-1,4(2 H,5 H)-dione]} are also commonly adopted as channel materials of synaptic devices that emulate the tactile systems^[23,37].

2.2. Inorganic-based tactile systems

Inorganic materials also offer diverse platforms for neuromorphic tactile systems. In contrast to the organic materials, inorganic materials have higher stability, better electrical performance, good process compatibility, and diverse functional properties^[38].

Carbon-based materials including graphene, carbon nanotubes (CNTs), and reduced graphene oxide can be classified as inorganic materials. They have high electrical properties and good stability along with mechanical flexibility, which makes them suitable material candidates for tactile systems^[39]. For instance, Chun et al. reported a graphene-based sensor array for mimicking the SA receptors^[40]. Here, the graphene was used as a form of nanoplatelets, exhibiting piezoresistive response under vertical pressure. In addition, CNT-based tactile systems have been frequently reported^[19,41–45] owing to the stability, high sensitivity, and flexibility of CNTs. CNTs are generally divided into single-walled carbon nanotubes (SWCNTs) and multi-walled carbon nanotubes (MWCNTs), and they are both widely used for tactile systems. Utilizing the high electrical conductivity and mechanical flexibility of MWCNTs, a simple and cost-effective tactile sensor could be established (Figures 2(c) and (d))^[19]. With the aid of ML algorithms, skin functions including letter writing, sliding direction recognition, and omnidirectional strain perception were also achieved.

Meanwhile, emerging inorganic materials such as MXene, transition metal dichalcogenides, and liquid metals are also considered promising materials for neuromorphic sensors and synaptic devices^[46,47]. Specifically, MXene is currently regarded as a highly promising material for sensing devices owing to its high electrical conductivity, large specific surface area, and water dispersibility. To date, various tactile sensors based on MXene have been reported^[22,48–51]. Tan et al. demonstrated a MXene-based tactile sensor which converts the detected pressure information into light pulses^[22]. Through this conversion, Morse code and object movement recognition task were successfully accomplished. Tactile near-sensor computing was also reported by Huang et al. with all MXene-based devices^[51]. In detail, MXene-based pressure sensor array and flexible MXene-based memristor array were integrated. Here, highly conductive MXene nanosheets were used for the sensing layer, while the remarkable mechanical properties and surface functional group adjustability of MXene enabled their utilization for the active layer in memristors. The proposed system obtained high recognition accuracy of handwritten digits (93.21%) and human motion (97.96%), demonstrating the potential for real-time monitoring systems utilizing the signals collected by sensor array and processing them by memristor-based ANNs. Liquid metals also possess unique advantages compared to other sensing materials, making them highly appealing for tactile sensors^[52–56]. Particularly, liquid metals such as gallium-based metals demonstrate excellent electromechanical properties, leading to high reliability in tactile sensors. Eutectic gallium indium (EGaIn) is one of the most widely used liquid metals for sensing devices. A bilayer soft sensor composed of oxidized EGaIn and bare EGaIn was presented by Kaneko et al., exhibiting a wide sensing range with low hysteresis and high stability^[52]. Moreover, the flexibility, fluidity, and low density of liquid metals make them highly desirable for flexible triboelectric sensors. The corrosion resistance of liquid metals also allows them to be utilized for underwater sensors^[57,58]. Li et al. reported a liquid metal-based underwater triboelectric palm-like tactile sensor, coupled with underwater robot gripper^[56]. The device consists of a flexible shell, cover, support, and a liquid metal-based triboelectric sensor. When the flexible shell is deformed by external stimuli, the hydrogel and the liquid metal in the sensor are separated from each other, thus generating electrical signals. The signals provide mechanical feedback for underwater robot grippers, resulting in object shape and hardness distinguishing accuracy of 99.75% and 100%, respectively.

Additionally, by leveraging the piezoelectricity or piezoresistivity of metal oxides including zinc oxide (ZnO) and perovskite oxides, various works on neuromorphic tactile sensory systems have been reported^[59–61]. In the case of ZnO, the zinc and oxygen ions in the crystal lattice can be displaced upon the application of mechanical stimuli, which triggers a change in the polarization state. For example, Kumar et al. reported a ZnO-based piezoelectric synapse capable of *in situ* touch sensing^[59]. Since various metal oxides can be fabricated via complementary metal oxide semiconductor (CMOS)-compatible process technology, util-

izing metal oxides can offer a significant advantage in terms of fabrication process and commercialization.

Overall, the key functions of biological mechanoreceptors could be emulated by neuromorphic tactile systems utilizing a variety of materials. Both organic and inorganic materials provide distinct advantages and shortcomings, which are in a trade-off relationship. Organic materials allow facile fabrication along with high biocompatibility and mechanical flexibility, which makes them more suitable for e-skin systems and wearable devices. On the other hand, inorganic materials have stable and diverse functional properties, resulting in better electrical performance. Nevertheless, for the development of advanced neuromorphic tactile systems, it is crucial to mitigate the drawbacks of each material while maintaining its strengths.

3. Neuromorphic auditory sensors

Human audition occurs through a series of complex processes. Initially, the outer ear collects the soundwaves from external surroundings^[62]. The soundwaves are converted to a form of mechanical vibration by the eardrum, which is then transformed into electrical signals. The transformation occurs when the hair cells in the cochlea bend against the tectorial membrane, thus opening the cation channels leading to a generation of action potentials. The action potentials propagate along the auditory nerves, finally reaching the brain.

Neuromorphic auditory sensory systems are inspired by the above biological auditory system. To date, various sensing materials and manufacturing methods have been explored for the fabrication of biomimetic auditory systems. Since neuromorphic auditory systems aim to emulate the mechanoreceptors, the sensor part of the device must be reactive to mechanical stimuli associated with sound waves. These stimuli include sound pressure, frequency, resonance effect, and sound onsets, which is why most artificial synaptic devices require the aid of external acoustic sensors for the sensing. Therefore, in this section, neuromorphic auditory systems are classified according to their manufacturing processes, rather than the core material of the system (Table 1).

3.1. Solution-based fabrication

Solution-based processing of various nanomaterials and thin films has been utilized for a long time. Solution processing encompasses a wide range of benefits, including cost-effectiveness, facile large-area fabrication, applicability of printing process, and acquirement of diverse material properties via concentration control. Since the artificial sensory systems have a large scale, the solution-based process can be a viable strategy for the fabrication. In this regard, solution-processed materials have widely been used for the development of auditory sensors. Various methods of solution processing have been developed throughout history, and in this section, we provide a review of recent reports of artificial auditory systems based on solution-based manufacturing processes^[63–67].

3.1.1. Evaporation-based techniques. Among several solution processes, the evaporation-based technique is the most common method. Evaporation-based technique refers to the synthesis of a certain material by evaporating the droplet of the solution in various ways. One of the most representative methods of evaporation-based technique is spin-coating. In this process, the solution is dropped on the surface of the substrate, which is then spun at high speeds, typically from few hundred rotations per minute (RPM) to few thousand RPM. During the spinning process, the solution spreads outward by the centrifugal force and the solvent evaporates, finally leaving a thin film. Gou et al. utilized a pyramid structure Si mold to form a tight and uniform conductive network of MXene with the spin coating method^[26]. On the pyramid structure Si mold, PDMS solution was spin-coated and a polyethylene (PE) film was laminated on top of the PDMS to peel off the PDMS form from the Si mold. Afterward, a MXene solution was spin-coated on the pyramid structure PDMS substrate, finally leaving a MXene-PDMS-PE structure. Here, the established structure was used as an artificial eardrum. For the sensing, the MXene initially senses the sound pressure produced by the speaker, achieving the first-stage enhancement. Subsequently, the bottom micro-pyramidal PDMS layer promotes the second-stage enhancement of sound sensing. Utilizing the two-stage amplification process, the artificial eardrum exhibited a high sensitivity of 62 kPa^{-1} and a low detection limit of 0.1 Pa. Furthermore, a high accuracy of 95% was achieved in human voice recognition test, indicating the acquisition of high overall performance via solution-based fabrication process.

3.1.2. Direct patterning techniques. Additionally, for much precise patterning of solution-processed materials, a direct patterning technique can be utilized. Inkjet printing method is a typical example of direct solution patterning. For instance, Bolat et al. reported printing of gate dielectric of a synaptic transistor with an AlO_x ink^[25]. Here, the AlO_x dielectric served as a charge-trapping layer, enabling the emulation of synaptic functions such as PPF and STDP. Through the obtained synaptic functions, an acoustic response system that can respond to all audio frequencies (20 Hz to 20 kHz) was established. Screen printing is another type of direct patterning method that has distinct advantages in terms of print resolution, pattern deposition, and substrate choice^[68,69]. This method does not require additional pre- or post-processes like photolithography. Only one step, in which the printable material is deposited via a stencil, is needed to form a patterned layer on a substrate. An organic electrochemical synaptic transistor array based on poly(3-hexylthiophene) (P3HT) and ionic-gel dielectric was reported by Xu et al., demonstrating neuromorphic sound localization^[70]. Here, P3HT film was prepared by evaporation-based self-assembly, and ionic-gel solution was coated on the gate electrode and channel by screen printing method. For the sound localization, head-related transfer functions dataset was utilized, where the normalized mean square error was reduced by 37.5% from the untrained period.

3.2. Combination of vacuum process with other fabrication methods

Conventional vacuum deposition-based process with photolithography is also a widely used fabrication method for artificial sensory systems, due to their high CMOS compatibility and scalability^[71–75]. Vacuum deposition processes are frequently coupled with other fabrication methods such as the transfer methods^[76,77]. For instance, Seo et al. demonstrated an artificial vdW hybrid synaptic transistor for acoustic pattern recognition task utilizing the CMOS technology with mechanical transfer method based on adhesion energy engineering^[24]. In this report, low-dimensional tungsten diselenide (WSe_2) and molybdenum disulfide (MoS_2) flakes were transferred onto *h*-BN via a residue-free transfer method. This method utilizes the difference in adhesion energy between the substrate for transfer and the layer after the transfer. When the flakes on the substrate contact a layer that has a stronger adhesion energy with the flakes, the flakes are picked up from the substrate and attached to the counter layer^[78]. Through this process, a clean interface without residues can be obtained. After the mechanical transfer, the pre- and post-synaptic terminals were vacuum-deposited and patterned by the photolithography process. The fabricated WSe_2 and MoS_2 hybrid channels served as the potentiation channel and depression channel, respectively (Figures 3(a) and (b)). To demonstrate the neuromorphic applicability of the vdW hybrid synaptic device, an acoustic pattern recognition task was carried out, based on the acquired linear and symmetric conductance-update characteristics (Figures 3(c)–(g)). Here, the vocal signals were converted into acoustic patterns, by recording and sampling the sound signals. Then, the processed information was transformed into an acoustic image. After training the images through a hardware neural network, 93.8% of acoustic pattern recognition accuracy was obtained. Yun et al. reported a self-aware artificial auditory system by connecting a TENG and a bi-stable resistor (biristor)^[27]. Here, the TENG was utilized both as an acoustic sensor and a current source, while the biristor served as a spiking neuronal device. For the fabrication of TENG, fluorinated ethylene propylene (FEP) film was placed between two copper electrodes. Eight spacers were used to separate the film from the top electrode, mechanically supporting the total structure at the same time. For enhancing the sensitivity of FEP film for different air pressure levels, micro-to-nano structures were created on the film via plasma etching process using a polymer etcher. Microelectromechanical system (MEMS)-based acoustic sensors also occupy a portion in neuromorphic acoustic sensors^[79,80]. MEMS-based sensors are fabricated via vacuum process coupled with micromachining technologies such as surface micromachining, high-aspect-ratio micromachining, and bulk micromachining techniques^[81]. These methods have distinct advantages in terms of designing complex and miniaturized mechatronic systems using batch fabrication. As an acoustic sensor, MEMS-based sensor serves the role as an artificial cochlea, which is coupled with additional synaptic devices or software-based ML techniques for realizing neuromorphic auditory applications. For instance, Lenk et al.

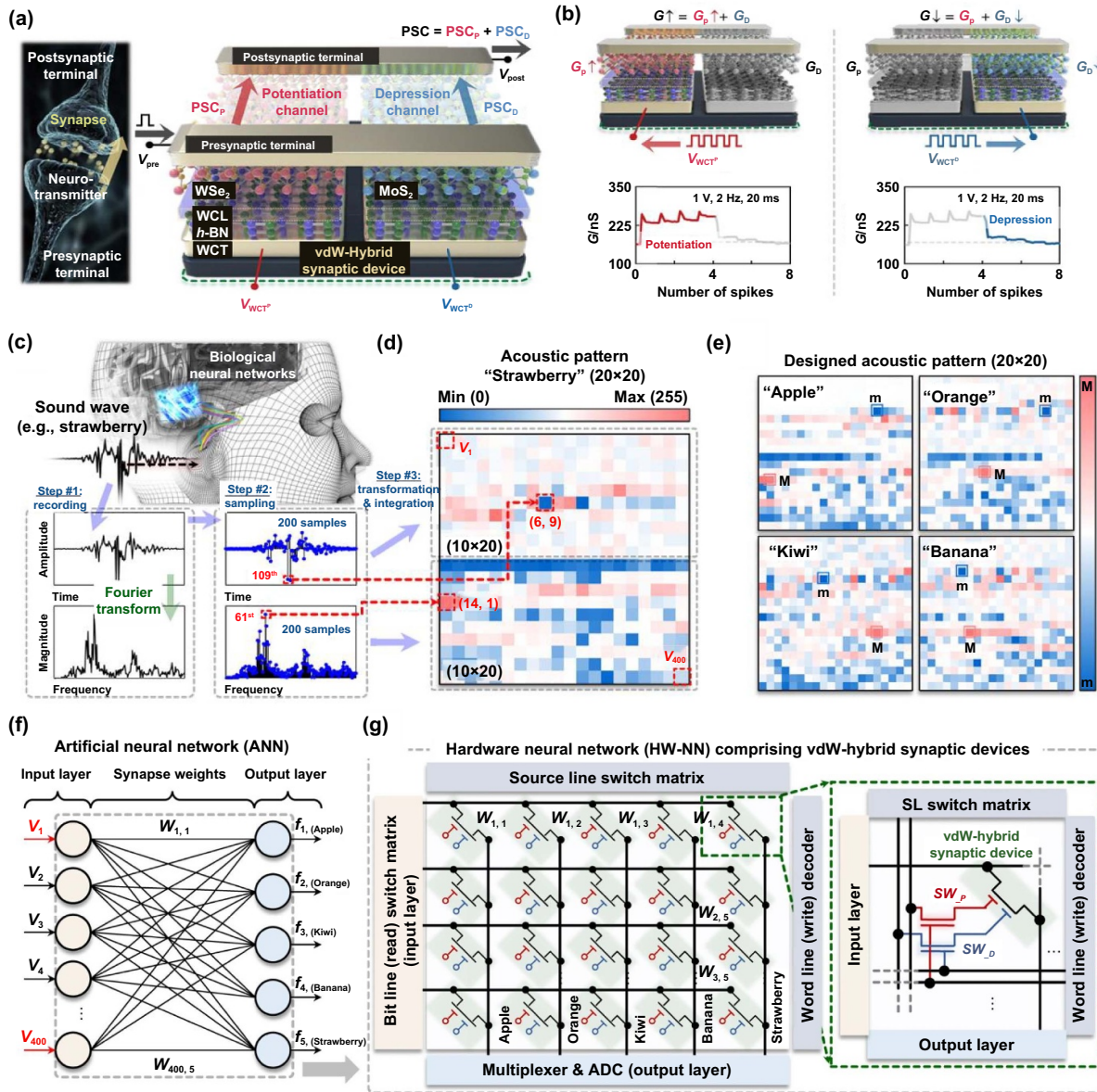


Figure 3. Neuromorphic auditory system utilizing van der Waals (vdW) hybrid synaptic devices. (a) Comparison between the biological synapse and the vdW-hybrid synaptic device. The device consists of potentiation and depression channels. (b) Potentiation and depression states obtained via four spikes. (c) Acoustic pattern generation process starting from recording, sampling, to transformation and integration. (d) The generated 20 × 20 acoustic patterns. Here, each pixel has a grayscale value ranging from 0 to 255. (e) Acoustic patterns indicating ‘apple’, ‘orange’, ‘kiwi’, and ‘banana’. (f) Illustration of single-layer ANN comprising 400 input neurons and 5 output neurons connected via synapses. (g) Hardware neural network composed of vdW-hybrid synaptic devices, capable of carrying out acoustic and Modified National Institute of Standards and Technology (MNIST) digit pattern recognition tasks. Reproduced from^[24]. CC BY 4.0.

presented a neuromorphic auditory system utilizing an adaptive MEMS cochlea with integrated real-time feedback^[79]. The proposed system achieved sensing properties comparable to that of mammalian cochlea and dynamical adaptation of the system was enabled by changing the feedback strength depending on the sensing amplitude.

Overall, both solution- and vacuum-based processes have been extensively utilized for the fabrication of artificial auditory systems and can be hybridized with various fabrication methods. Both procedures possess solid advantages,

making them suitable for the production of neuromorphic devices. Nevertheless, there are still several key challenges for both types of processes. In the case of the solution process, the ambient stability and relatively low electrical performance can be an issue for artificial sensory systems. On the other hand, the biocompatibility and cost issues might be a problem for vacuum-based technology. Thus, research on the fabrication technology itself must not be overlooked to witness another breakthrough in neuromorphic sensory systems.

4. Neuromorphic olfactory and gustatory sensors

The perception of smell takes a large part in the survival strategy of numerous organisms. Although humans rely more on vision and audition, humans can still distinguish thousands of different odors. Specifically, human olfaction is mainly governed by chemoreceptors in the nose, which detect airborne chemicals. Odor molecules in the air consist of various chemical molecules, and they can bind to specific olfactory receptors that exist in the upper nasal cavity^[82]. Afterward, electrical signals are generated by olfactory neurons and travel along the axons. The signals then reach the olfactory bulb of the brain and are recognized. In a similar manner, gustation is also dominated by the chemoreceptors in the taste buds on the tongue. When a human intakes certain food or drink, the chemical molecules contained in the food can couple with different types of taste receptors. This reaction can generate action potentials, finally enabling the five main taste sensations: sweet, sour, salty, bitter, and umami.

Utilizing these concepts, various artificial olfactory and gustatory sensor systems have been introduced (Table 2). These systems primarily aim to emulate the ability of chemoreceptors by using sensors that can distinguish different types of biochemical molecules. Despite their successful sensing performance, there is still room for advancing the in-sensor computing technology by creating a bio-hybrid interface. In this context, we will more focus on the integrated sensory systems rather than a single sensory system.

4.1. Artificial olfactory systems

The history of artificial olfactory systems is rather short compared to tactile or vision systems. The first ever artificial olfactory system was reported in 1982^[92], as far as we found, mimicking the odor detection and the subsequent information processing system. The key to the emulation of biological olfaction is the differentiation of chemical molecules. However, most materials capable of gas-detection are not suitable for artificial synaptic devices. In this regard, separate synaptic devices are additionally employed for fabricating neuromorphic olfactory systems. Thus, in this section, we will discuss the recently reported artificial olfactory systems categorized by different device structures since the structure affects the synaptic functions of the neuromorphic sensory system. In this section, we will discuss the recently reported artificial olfactory systems categorized by different device structures.

4.1.1. Two-terminal synaptic devices. Two-terminal synaptic devices have been extensively studied due to their simple structure and operating mechanism along with the potential of low power consumption. Chu et al. reported a synaptic diode with OSCs/amorphous indium-gallium-zinc-oxide (IGZO) lateral p-n heterojunction structure for power-efficient gas sensing system^[87]. Here, three types of OSCs including 2,7-dioctyl[1] benzothieno[3,2-b][1]benzothiophene (C8-BTBT), dinaphtho[2,3-b:2',3'-f]-thieno[3,2-b]thiophene (DNNT), and pentacene were adopted, and since they are placed as an upper

layer, they can interact with gas molecules in the air. In specific, synaptic behaviors such as inhibitory postsynaptic current (IPSC) and PPD can be induced by ammonia gas through the charge-dipole interaction which diminishes the overall current. To explore the applicability of ammonia gas sensing, the real-time detection and analysis of ammonia in the exhaled breath of human was simulated, suggesting the potential of the synaptic diode for human health monitoring. Olfactory systems with memristors were also reported by Chun et al. (Figure 4(a))^[83]. Metal oxide NRs including TiO₂ and NiO were used as the active layer of the memristor, while serving as the gas sensor as well. After the initial memristive switching, the redox reaction of the proposed chemi-memristive gas sensor is influenced by external gas molecules, leading to a current change (Figures 4(b) and (c)). For the potential application, an olfactory system that can monitor the history of input gas was demonstrated. Further, an accuracy of 92% was achieved in MNIST pattern recognition test through the linear and symmetric conductance modulation properties, indicating the simultaneous functioning of gas-sensing and synaptic information processing (Figure 4(d)). The above olfactory systems have successfully demonstrated various single gases, but failed to discriminate certain types of gas in a mixed environment. Thus, to better emulate the biological olfactory system, neuromorphic olfactory systems capable of mixed-gas detection were reported as well^[93,94]. Especially, Wang et al. reported a novel monolithic 3D olfactory sensor array chip, including 10 000 individually addressable sensors and capable of distinguishing 24 kinds of mixed gas simultaneously^[94]. Vertical metal oxide nanotubes were fabricated on a porous alumina membrane substrate with atomic layer deposition (ALD) and a multi-step suspended mask-assisted sputtering. With the aid of various ML techniques including convolutional neural network (CNN), accuracy of 99.04% was achieved for single gas discrimination of eight gases with different concentrations and humidity. For mixed-gas detection, 96 kinds of gas mixtures with different concentrations were distinguished, where the response of the sensors changed in proportion to concentration. Above all, 24 objects with distinct odors were real-time classified, and the fabricated olfactory chip was integrated into a robot, taking a huge step towards the development of sophisticated humanoid robot with biomimetic olfactory functions.

Apart from the introduced sensory systems, two terminal devices are widely implemented in artificial olfactory systems^[95], owing to their unique advantages. However, the intrinsic stochasticity of two terminal devices and the limited range of conductance tunability remain crucial challenges for securing high device reliability and neuromorphic performance. To address these issues, the employment of three-terminal devices can be a viable alternative.

4.1.2. Three-terminal synaptic devices. Three-terminal synaptic devices are generally based on the transistor structure having gate, source, and drain electrodes. Among various types of three-terminal devices, OECTs occupy a large portion^[84,96–98]. Deng et al. demonstrated a flexible and biomimetic olfactory synapse based on OECT with porous

Table 2. Summary of neuromorphic olfactory and gustatory systems.

Year	Material	Manufacturing	Structure	Applications	Recognition accuracy	References
2023	Metal Oxide TiO ₂ , NiO NRs	Vacuum process	Two terminal structure	Gas sensing MNIST digit pattern recognition	92.76%	[83]
2023	Organic material PEDOT:PSS	Solution process	Three terminal structure	Health monitoring system	N/A	[84]
2024	Human olfactory receptor Organic material ion gel, organic semiconductor	Solution process	Two terminal structure (sensor) Two terminal structure (neuron)	Odor recognition Gas detection	91.6%	[85]
2023	Inorganic material Si NW	Vacuum process	Three terminal structure	SNN Gas classification	N/A	[86]
2022	Metal Oxide IGZO Organic material Pentacene, DNTT, C8-BTBT	Vacuum process	Two terminal structure	Real-time gas detection	N/A	[87]
2022	Metal Oxide SnO ₂ NW Organic material chitosan ion gel	Solution process	Three terminal structure	Health monitoring and alarming functions for excessive intake	N/A	[88]
2024	Organic material Polymer (PTFE, FEP, PE, PDMS)	Solution process	Multiterminal structure	E-tongue Liquid classification	> 92.7%	[89]
2022	Human taste receptor TIR2 VFT Inorganic material CNT	Solution process	Three terminal structure	E-tongue	N/A	[90]
2023	Inorganic material Graphene 2D material MoS ₂	Vacuum process Transfer method	Chemi-transistor (sensor) Memtransistor (synapse)	Feeding decision Humanoid AI	N/A	[91]

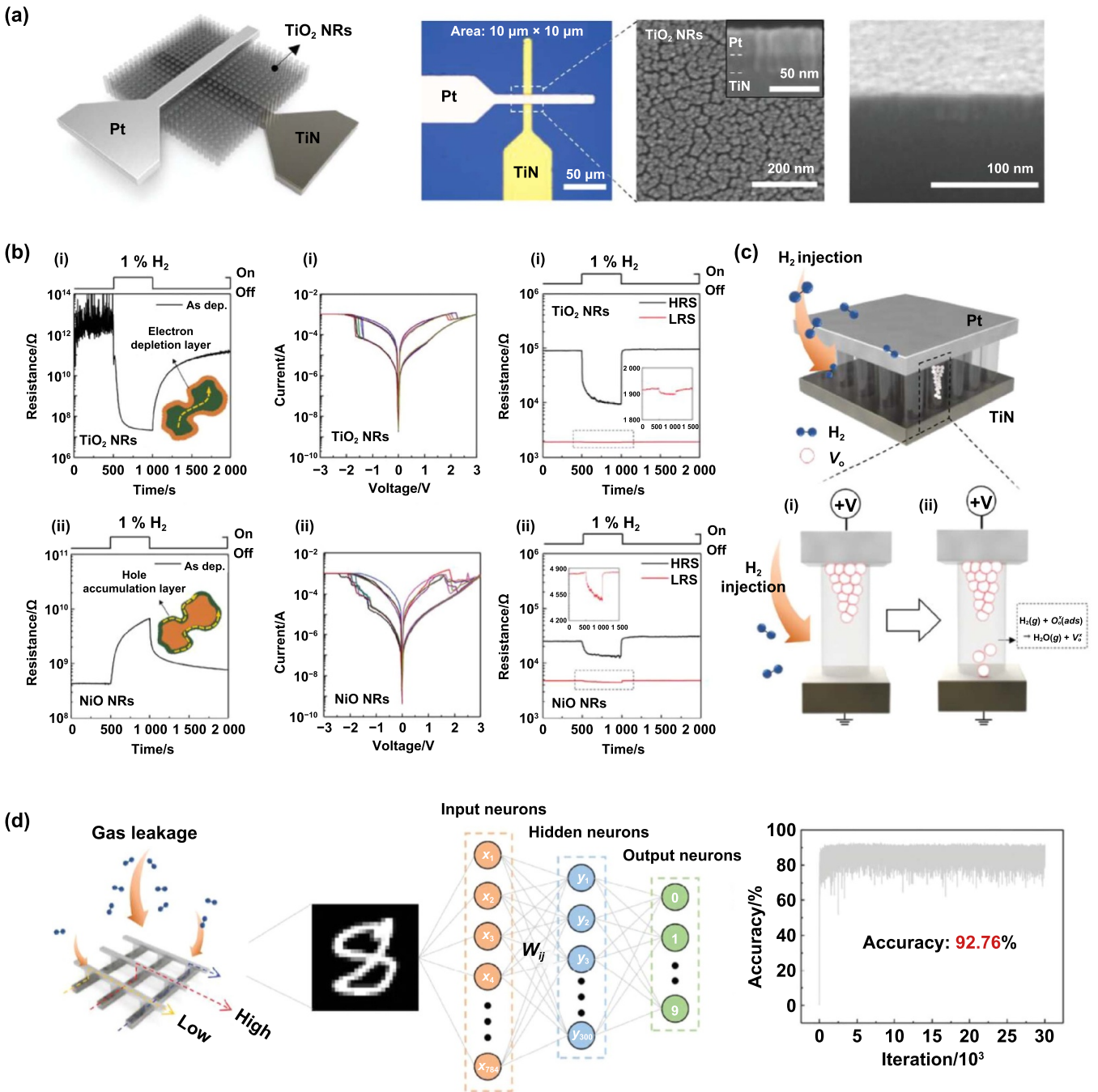


Figure 4. Illustration of neuromorphic olfactory system based on chemi-memristive device. (a) Schematic diagram of chemi-memristive device (Pt/TiO₂ nanorods (NRs)/TiN) with a crossbar structure. The right images show the optical microscopy (OM) image and cross-sectional SEM images of TiO₂ NRs. (b) Response curves of TiO₂ and NiO NRs after exposure to H₂ gas. The I-V curves of TiO₂ and NiO NR-based devices are presented as well. (c) The response of the device towards H₂ gas. Injection of H₂ gas triggers the generation of oxygen vacancies, resulting in the increase of conductivity. (d) MNIST-based simulation system for inferring gas generation location. The accuracy of 92.76% was acquired in the pattern recognition test. Reproduced with permission from^[83]. CC BY-NC-ND 4.0.

solid polymer electrode (SPE) inspired by human breath (Figures 5(a) and (b))^[84]. The device was based on the conducting polymer, poly(3,4-ethylenedi oxythiophene) doped with poly(styrene sulfonate) (PEDOT:PSS), exhibiting high selective sensitivity for H₂S over other gases. Specifically, when the device is exposed to H₂S, the ionic association occurs between H₂S and SPE. This, in turn, weakens the electrostatic interactions between the cations and anions in the SPE. Hence,

the cations can be injected into the PEDOT:PSS channel, resulting in the de-doping process and reduction of channel current. Through this process, the exposure of H₂S gas was able to mediate the synaptic plasticity of the device creating a neuromorphic olfactory system. Since H₂S can be found in spoiled food, the proposed system was also successfully exploited as a food monitoring system that detects rotten eggs, suggesting that the system can be utilized for real-life applications.

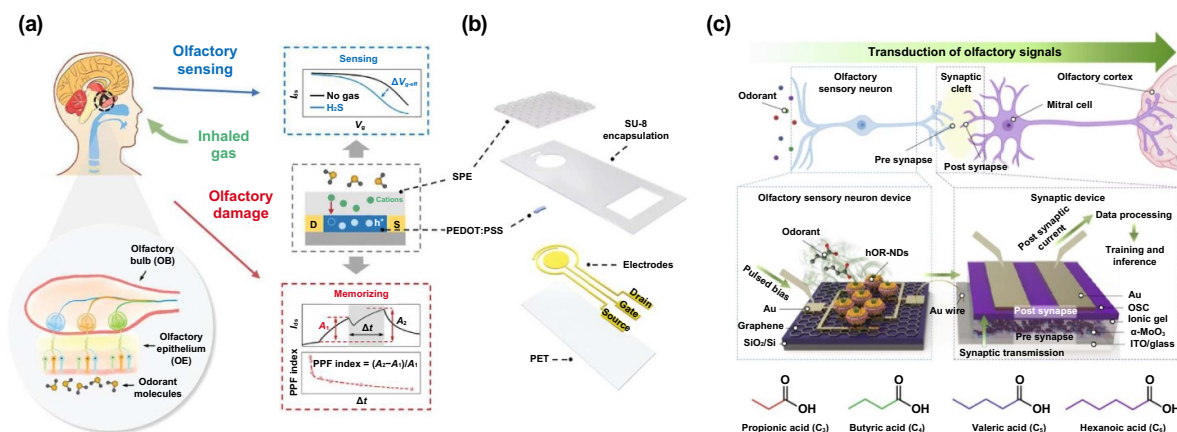


Figure 5. Two different neuromorphic olfactory systems each utilizing an OECT and hOR coupled with synaptic device. (a) Schematic illustration about the concept of the neuromorphic olfactory synapse. The exposure of H₂S gas triggers a threshold voltage shift in the OECT, enabling the sensing of the gas. Further, the memorizing function of the device can be utilized to emulate the olfactory damage induced by the overexposure of H₂S gas. (b) The device structure of the synaptic device. A transistor with PEDOT:PSS channel was fabricated on a flexible polyethylene terephthalate substrate, subsequently encapsulated by an SU-8 layer. (a) and (b)^[84] John Wiley & Sons. © 2023 Wiley-VCH GmbH. (c) Comparison between human olfactory system and the proposed artificial olfactory system. Three types of hOR NDs were purified from *E. coli* and transformed into stable structures, which were then used as an olfactory neuron. Here, the neuron was additionally connected to the artificial synaptic device to process the acquired olfactory information. From^[85]. Reprinted with permission from AAAS.

More recently, an integrated artificial olfactory system comprising an artificial synapse and human olfactory receptors (hORs) was reported (Figure 5(c))^[85]. In this approach, the hOR-functionalized extended gate corresponds to an olfactory sensory neuron and the organic synaptic transistor corresponds to the artificial synapse. For the successful incorporation of hORs into a lipid bilayer, the nanodisk (ND) assembly technique was utilized. Three types of hORs-hOR51E1, hOR51E2, and hOR52D1-were constructed into NDs and functionalized on a graphene-extended gate. When the NDs were exposed to a certain odorant, the hORs underwent a modification, resulting in the change of resistance. This change triggers a transduction of signal, which is transmitted to the pre-synaptic electrode of the OECT, modulating the channel conductance. Finally, the PSC changes, enabling the detection of odorants. Through this process, four types of short-chain fatty acids could be successfully identified, highlighting a high potential for the development of biocompatible olfactory systems.

Typical FETs are also widely used for neuromorphic sensory systems. Lee et al. established an in-sensor computing system using a Si-NW FET which has a similar structure to the fin-shaped FET^[86]. In this work, two different catalytic metal nanoparticles of palladium and platinum were formed on top of the exposed Si-NW. These nanoparticles can detect H₂ and NH₃ gas, rendering the FET as a gas sensor. When the nanoparticles react with the gas, the threshold voltage of Si-NW FET shifts, thus generating spike signals as an artificial sensory neuron. The generated spikes were utilized for spiking neural network (SNN) processing and the two types of gases could be successfully classified. Mimicking the sense of olfaction is a challenging task. Although various researches have paved the way for the development of olfactory systems, the progress is still in an early stage. One of the main obstacles to constructing biomimetic olfactory system is the difficulty

in creating hundreds of different types of gas-sensing materials. Living organisms can detect countless types of odors simultaneously through the assistance of millions of olfactory receptor neurons, which is not an easy feature to emulate. Further challenges include the difficulty of shortening the response and recovery time for odors, suggesting that more effort must be devoted to the development of truly biomimetic olfactory systems.

4.2. Artificial gustatory systems

Quite similar to the artificial olfactory systems, research of artificial gustatory systems has not been extensively explored yet, compared to other sensory systems. Since artificial gustatory systems mimic biological chemoreceptors, the sensor must be reactive to different types of chemical biomolecules. However, it is a challenging task to fabricate a chemical-sensing material that can be used for the active layer of synaptic devices. In this regard, recent studies have demonstrated integrated types of gustatory systems, where a majority of gustatory sensors are connected to external synaptic devices. Thus, in this subsection, integrated neuromorphic gustatory systems are introduced, based on two types of integration methods. Few reports of monolithically integrated gustatory systems exist. Monolithic systems have strong points in terms of system size reduction, power consumption, and facile transfer of sensory information. However, the intrinsic properties of chemical sensors demonstrate low potential as a synaptic device, thereby limiting the performance and the range of applications. On the other hand, heterogeneous system can integrate separate high-performance sensor and synaptic device, boosting the total performance of the integrated system. However, heterogeneous systems consume higher power

and fabrication cost, and might have interface issues when integrating a sensor and an artificial synapse.

4.2.1. Monolithic integration. First, we introduce few representative examples of artificial gustatory systems with monolithic integration. Yang et al. utilized a SnO₂ NW artificial synaptic device with a chitosan-based ion-gel gate dielectric (Figure 6(a))^[88]. Regarding the sensing mechanism, the ionic conductance of ion-gel sensor changed under various NaCl concentrations. Subsequently, cations such as Na⁺ and H⁺ can be captured and accumulated on the SnO₂ NW channel under an electric field, leading to a change in postsynaptic current values. Upon removing the electric field, the cations diffuse along the concentration gradient, where the process can be defined as the taste memory. Since the appropriate salt content in body is crucial to survival, the proposed gustatory system can further be utilized for health monitoring (Figures 6(b) and (c)). To realize the salt intake monitoring function, the artificial gustatory system is also integrated with an effect-executive unit, which is triggered by the information processed from the synapse part of the device. Further, another type of monolithically integrated gustatory system with electrolyte-gated vertical organic field-effect transistors (VOFETs) capable of gustatory sensing was reported^[99]. For the VOFETs, P3HT was inserted between the source and drain electrodes, which was defined as the channel layer. For the electrolyte, the ionic liquid [EMIM][TFSI] was utilized, serving the role as the weight-control layer. Here, the ionic liquid also plays the role of human saliva. Since the electrolyte is highly biocompatible and could form an electric double layer under a gate voltage, the channel conductance could be modulated by migration and subsequent injection of the mobile ions into the permeable semiconductor channel layer. This process is highly similar to the modulation of biological synaptic plasticity. For the emulation of human gustation, two types of acetic acid (AA) with different concentrations were dropped to a 3 × 3 array of VOFETs, with a fixed appliance of single electric pulse to detect the current change. When the device was subjected to AA with higher acid concentration, higher current change was observed. Repeated acid stimulation also elicits cumulative pain responses, demonstrating human synaptic behavior to repeated acidic stimuli. These types of monolithically integrated artificial sensory systems have distinct advantages in terms of device size optimization and power consumption, suggesting the need for the development of sensory systems with monolithic integration.

4.2.2. Heterogeneous integration. Heterogeneous integration of artificial gustatory system typically includes a sensory device for sensing taste, and a synaptic device for processing the sensed taste information. For instance, Jeong et al. developed an artificial E-tongue by fabricating T1R2 venus flytrap (VFT)-immobilized carbon nanotube FET with floating electrodes, which can detect sweet substances and discriminate them from other mixed taste substances^[90]. T1R2

VFT of the sweet taste receptor is known as a primary ligand-binding domain for sweet tastants, and in this work, polymerase chain reaction method was utilized for the gene cloning of T1R2 VFT. Afterward, the T1R2 VFT was immobilized on the floating electrode by dropping the T1R2 VFT solution on the channel region of the sensor. For the sensing mechanism, Schottky barrier modulation induced by the change of work function of the floating electrode was implemented. The binding of sweet substance to T1R2 VFT triggered charge redistribution, which in turn changed the work function of the floating electrode. This caused the current change of the device, allowing the detection of specific substances. Triboelectric-based sensors are gaining interest since they can offer the possibility of self-powered sensing and portable packaging of devices, emphasizing more research in this field. Recently, Liu et al. reported a bioelectric integrated triboelectric E-tongue with high taste classification accuracy (Figure 6(d))^[89]. Four types of triboelectric polymer films were integrated into a single glass slide chip. When a droplet of a sample contacts the sensor surface and slides, the charge state of the polymer film changes (Figure 6(e)). As the droplet slides downward, the charge transfer and charge accumulation process repeatedly occur until the droplet falls of the sensor. Subsequently, a charge attraction within the connected metal electrodes occurs through electrostatic induction, leading to a generation of induced current. The acquired data was then coupled with an external AI software for the classification of different samples (Figure 6(f)). As a result, high accuracy of 100%, 98.2%, and 97% was obtained for chemical solutions, environmental samples, and four types of teas, respectively. This work highlighted the advancement of liquid sensing technology and offers the possibility for the development of E-tongue systems with diverse sensing mechanisms.

Artificial gustatory systems in heterogeneous integration with high CMOS compatibility have also been presented. Han et al. reported an E-tongue that comprises of a gustatory sensor and a metal-oxide-semiconductor FET (MOSFET) which plays the role of an input neuron in the SNN system^[100]. Here, a pH-sensitive Al₂O₃ and sodium-sensitive sodium ionophore X were employed as the sour and salty taste sensors, which were connected to the MOSFET as an extended gate structure. When a certain biomolecule interacts with the sensing part, there occurs a change in the surface potential and surface charge of the sensor. Since the sensor part is connected to the gate of the MOSFET, the spiking frequency of the MOSFET changes, enabling the detection of flavor. Through this mechanism, two types of liquids were classified. Moreover, Ghosh et al. demonstrated a 2D-material based artificial gustatory system that mimics the adaptive human feeding behavior^[91]. For the sensory part, graphene-based chemi-transistor was utilized and a memtransistor with MoS₂ channel was used as a synaptic device. Specifically, the memtransistor served as an electronic gustatory cortex including the hunger neuron, appetite neuron, and feeding circuit. This research is differentiated from other works, in that they incorporated physiology and psychology, suggesting a new paradigm for gustatory emotional intelligence. Further, the two introduced

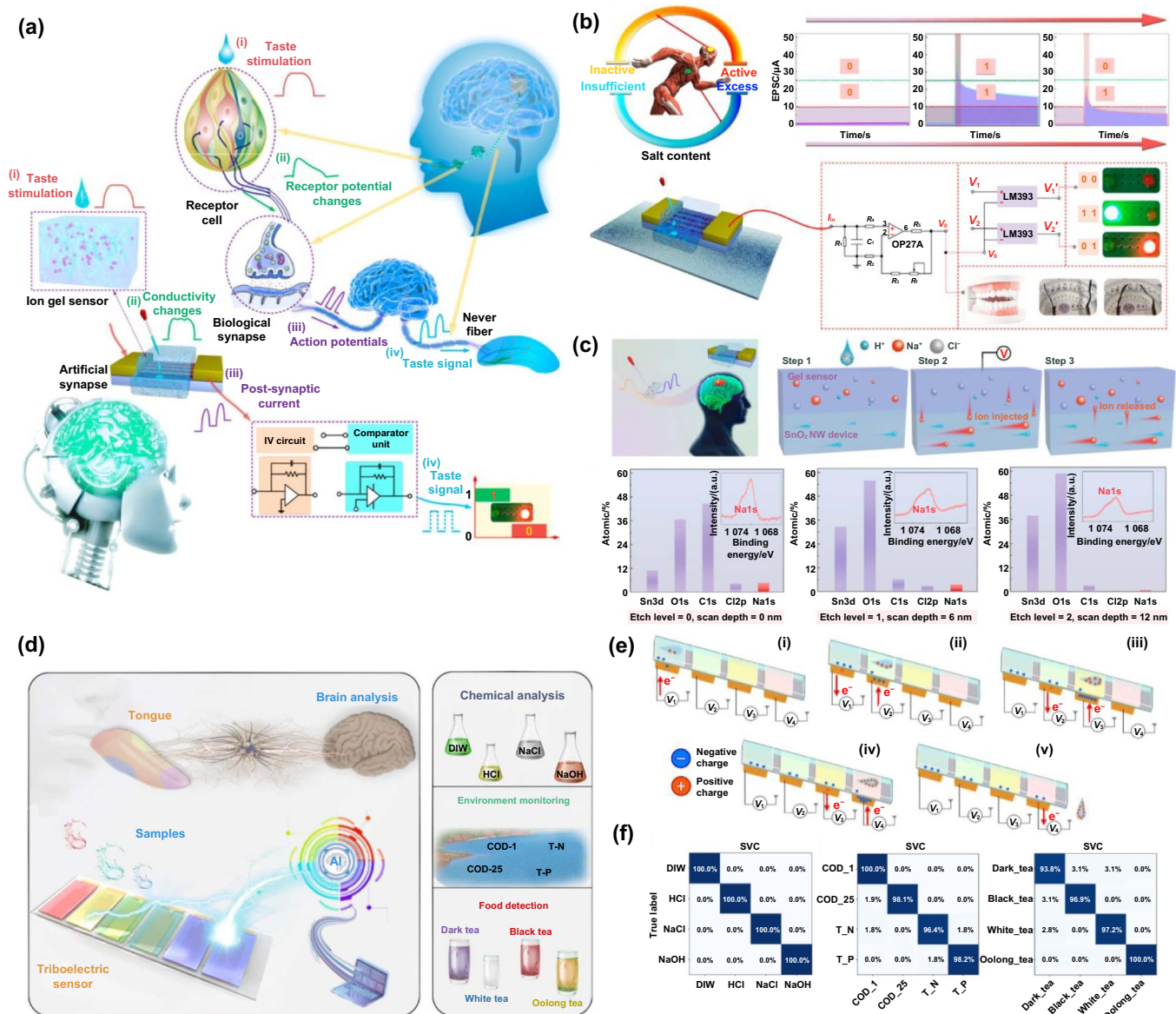


Figure 6. Neuromorphic gustatory system with various device architecture and sensing mechanisms. (a) Illustration of biological and artificial gustatory system. Together, the chitosan-based ionic gel sensor, SnO₂ nanowire (NW)-based artificial synapse, and an execution unit make up the neuromorphic gustatory system. In this approach, the sensor distinguishes the difference in the concentration of NaCl by controlling the inflow number of sodium ions. Afterward, the information is transmitted via the synaptic device, finally triggering the activity of the execution unit. (b) The construction of the gustatory system capable of health-monitoring and excessive-intake alarming functions. The graph on the right exhibits the post-synaptic current (PSC) evolution after addition of different NaCl solutions. (c) Working principles of the neuromorphic gustatory system. The bottom x-ray photoelectron spectroscopy patterns of SnO₂ layer indicate the difference in elemental distribution after Na⁺ injection. (d) Schematic diagram of the triboelectric gustatory sensor and the applications. (e) Main operating mechanism of the triboelectric E-tongue. (f) Classification results for chemical, environmental, and tea samples. (a)–(c) Reprinted (adapted) with permission from [88]. Copyright (2024) American Chemical Society. (d)–(f) Reproduced from [89]. CC BY 4.0.

systems were mainly fabricated via conventional photolithography along with vacuum deposition process, which is also a great advantage.

Overall, the above systems offer a great potential for future gustatory AI systems in that they do not require von-Neumann hardware components, hugely increasing cost and energy

efficacy. However, there are still challenges for achieving broader chemical sensing range and applying the gustatory systems to an actual humanoid AI system. To date, the reported neuromorphic gustatory systems are unable to truly mimic the biological gustation. Similar to the neuromorphic olfactory systems, gustatory systems require numerous sensors that

can react to countless different types of chemicals, which is a difficult task to be done. Deeper understanding of biological gustation and how the processing of the sensory information occurs must be preceded. The aid of advanced ML algorithms may also help realize real-time multi-flavor detecting sensors.

5. Neuromorphic vision/optoelectronic sensors and their applications

Humans gather information through external stimuli such as sounds, pressures, and odors as mentioned above, to perform functions such as learning and memorizing. Among these stimuli, over 80% of information is collected through the visual senses, indicating that the visual information is the most critical sensor modality in human cognition^[101]. Through vision, humans engage in communication, emotion recognition, and decision-making. Based on the understanding of biological mechanisms, extensive research has been conducted to translate the traditional vision sensors to those emulating the human vision system^[102,103]. In the human vision system, light enters the eye and traverses through the cornea and lens before converging onto the retina, where photoreceptor cells (rods and cones) transform the light into corresponding electrical signals^[104]. These signals are further pre-processed by the horizontal and bipolar cells and then facilitated by the ganglion cells. Then, they are conveyed to the brain's visual cortex via the optic nerve, where they are processed and integrated into meaningful visual experiences. The essential feature of bio-inspired artificial vision sensor is that the synaptic weight (conductivity) can vary or even be preserved in response to the incident light signal.

However, traditional vision sensors may have reached their limits due to issues such as large amounts of redundant data, latency in data processing, and high-power consumption, especially in implementing the retina-like functions^[105–107]. Moreover, with the advancement of AI in areas like robotics and autonomous driving, the demands for high acquisition of visual information have highlighted these problems further. As a result, the development of synaptic devices that mimic the neurobiological structure and functions of the retina, photodetectors with memory capabilities, and methods to directly modulate the synaptic weights using light signals are being explored to address these challenges and enhance the visual sensing technology. Such synaptic devices require characteristics that maintain the conductance long after the removal of light stimuli, known as the persistent photoconductivity (PPC) effect. Inspired by these synaptic functions, neuromorphic photonic devices composed of low-dimensional materials^[108–110], metal oxides^[111–113], ferroelectrics^[114,115], organic materials^[116–118], and perovskite photoactive materials^[119,120] have been extensively investigated recently. Based on the photosensitive properties of the above materials, it is facile to utilize the photoconductive effects to simulate the function of photonic synapse, which

has shown great potentials in image sensing and processing, color recognition, optoelectronic logic operations^[121–123]. Herein, we delve into several representative examples of neuromorphic vision sensors and optoelectronic devices (Table 3).

5.1. Bio-inspired neuromorphic vision/optoelectronic devices

In recent years, neuromorphic vision sensors have attracted considerable interest due to their enhanced capabilities in image sensing and processing, visual-assisted learning, and color recognition. Since the optical properties of photoactive materials determine the operating principles and the applications of biomimetic optoelectronic devices, we primarily focused on the usage of various photoactive materials. Therefore, in this subsection, we categorize the development of neuromorphic vision sensors according to the photoactive materials, including low-dimensional materials, metal oxides, ferroelectric materials, organic and perovskite materials, along with their fabrication processes and working principles.

5.1.1. Low-dimensional material-based optoelectronics.

Low-dimensional materials stand out as particularly promising materials for crafting photonic synapses, due to their robust light-matter interaction and the ability to tailor their bandgap flexibly^[136]. These materials, spanning through 0D^[108], 1D^[125,137], and 2D^[138] structures, cover a broad bandgap spectrum from ultraviolet (UV) to infrared (IR), making them versatile photoactive elements for bio-inspired photonic synapses. Among these, 0D materials—nanoscale entities where electron movement is restricted in all dimensions—demonstrate extraordinary physical and chemical characteristics, primarily attributed to pronounced quantum confinement effects^[139]. Quantum dots (QDs), a subset of 0D materials, have distinguished themselves as superior photoelectric substances due to their adjustable bandgap by the size, exceptional luminescent qualities, and decent stability^[140]. Zhang et al. unveiled an innovative retina-inspired image sensor that adeptly captures, pre-processes, and stores broadband visual information spanning from UV to near-IR (NIR) wavelengths^[124]. The sensor integrates a PbS QDs/pentacene heterostructure with a PbS QDs/poly(methyl methacrylate) (PMMA) photoresponsive charge trapping layer, capitalizing on the innate flexibility of the zero-dimensional (0D) QDs (Figure 7(a)). Under light illumination, photogenerated electrons are trapped in the PbS QDs/PMMA layer, while holes are injected into the pentacene channel, modulating the channel conductance. These processes enabled synaptic behaviors such as the excitatory post-synaptic current (EPSC) and LTP, replicating adaptive photo-response. Importantly, the retention time of trapped charges allowed the device to achieve non-volatile memory functions and adaptive photo-response over a wide spectral range of light. A sophisticated flexible array, designed to

Table 3. Summary of neuromorphic optoelectronic systems.

Year	Material	Manufacturing	Structure	Synaptic function	Applications	Recognition accuracy	References
2023	PbS QDs/PMMA	Solution process	Three terminal structure	EPSC, PPF, STP, LTP, STP-to-LTP transition	Contrast enhancement Image processing	N/A	[124]
2022	ZnO NW	Solution process	Three terminal structure	EPSC, IPSC, PPF, STDP	MNIST digit pattern recognition	92%	[125]
2023	Metal Oxide ZnO/MoO ₃	Vacuum process	Two terminal structure	EPSC, PPF	Image processing (CNN) MNIST digit pattern recognition	90%	[126]
2023	Metal Oxide TiO ₂ , IGZO	Vacuum process	Three terminal structure	STM, PPF, LTM	MNIST digit pattern recognition	90.3%	[127]
2021	Metal Oxide IGZO	Solution process	Two terminal (photoresistor)	STP, LTP, LTD, PPF	Hardware pattern training	86.82%	[128]
	Metal Chalcogenide CdSe, CdS	Vacuum process	Three terminal (synaptic transistor)		MNIST digit pattern recognition		
2022	PZT/SRO	Vacuum process	Two terminal structure	LTP, LTD	Pattern classification (ANN) Edge detection	N/A	[114]
2023	<i>a</i> -In ₂ Se ₃	2DMC transfer	Three terminal structure	LTP, LTD	Color recognition (CNN CIFAR-10)	93%	[115]
2022	P(VDF-TrFE)/Cs ₂ AgBiBr ₆	Solution process	Two terminal structure	EPSC, PPF	Image classification (RC) Motion detection	99.97%	[129]
2024	Inorganic material Cs _{0.05} MA _{0.15} FA _{0.8} PbI _{0.85} Br _{0.15}	Solution process	Two terminal structure	STP, LTP, LTD	ANN Image recognition (ANN)	97.8%	[130]
2023	ITZO/InP QDs	Solution process	Three terminal structure	PPF, STP, LTP	Visual adaptation MNIST digit pattern recognition	93%	[131]
2022	InP/ZnSe QD	Solution process	Three terminal structure	EPSC, PPF, STP, LTP	Image processing MNIST digit pattern recognition	91%	[132]
	SnO ₂ oxide semiconductor						
2023	Modified silk fibroin protein	Solution process Vacuum process	Two terminal structure	STP, LTP, LTD	Image processing High-level image recognition	97.3%	[133]
2023	Organic/2D molecular crystal (n-type TFT-CN ^(a) /p-type DTT-8 ^(b))	Solution process 2DMC transfer	Three terminal structure	EPSC, IPSC, PPF, STP, LTP, LTD	Motion detection	90%	[134]
2024	Organic material Poly (sulfobetaine methacrylate), 2-decyl[1]benzothieno[3,2-b][1]benzothiophene	Solution process	Three terminal structure	EPSC, PPF, STP, LTP, STM, LTM	RC for motion recognition	95.56%	[135]

^(a) TFT-CN: 2,2'-(5Z,5'Z)-5,5'-(furan-2,5-diylidene)bis(4-octylthiophene-5,2(5H)-diylidene)) dimalonon-itrile.^(b) DTT-8: π -conjugated dithieno[3,2-b:2',3'-d]thiophene derivatives.

replicate key functions of the human retina such as contrast enhancement, was constructed (Figure 7(b)). Notably, this array facilitates a dynamically adjustable image preprocessing capability, dramatically reduced the preprocessing time by approximately 80% under optimized gate voltage conditions, thereby harnessing gate-adjustable synaptic plasticity to enhance operational efficiency.

1D materials, characterized by their elongated, one-dimensional structure, exhibit unique electrical and mechanical properties that are advantageous for various engineering applications^[141]. One of the most widely studied 1D materials is the semiconducting NW, providing significant benefits in fields ranging from electronics to materials science due to their mechanical flexibility and process scalability^[142,143]. Shen et al. demonstrated a ZnO NW FET with a charge-trapping layer incorporated into the gate dielectric^[125]. The synaptic potentiation behavior was achieved through the PPC effect in the ZnO NWs. Under UV light illumination (wavelength of 365 nm), photogenerated electrons and holes are created. The desorption of oxygen molecules from the ZnO NW surface increases the carrier density in the channel, resulting in a significant increase in current, mimicking the EPSC. The gradual re-adsorption of oxygen molecules in dark enables the device to emulate synaptic decay, analogous to the STP. In contrast, synaptic depression is induced by applying electrical pulses to the gate electrode in dark. The gate-induced electric field drives electrons from the ZnO NW channel into the charge-trapping layer, which reduces the carrier density and thereby the channel current. This bidirectional modulation of synaptic weight, controlled by optical and electrical stimuli, closely resembles the synaptic potentiation and depression observed in biological systems. Additionally, by applying the ANN simulations, they achieved a recognition rate of over 90% in MNIST recognition tasks.

2D materials display remarkable and distinct electronic and optoelectronic properties, enabled by electrostatic control due to their ultrathin dimensions and unique band structures^[144]. Compared to the previously mentioned 0D and 1D materials, 2D materials demonstrate advantages in device fabrication and integration due to their planar structures^[139]. In optoelectronic devices based on 2D materials, the atoms within each layer are bonded covalently, allowing them to act as atomically thin channels without dangling bonds on the surface. The layers are held together by weak vdW forces^[145]. This distinctive structure enables electrons to be confined within the ultrathin channel and manipulated via an electric field. Therefore, extensive research has been conducted on various 2D materials, including MoS₂, and tungsten disulfide (WS₂). Ma et al. developed a monolithic chip based on a wafer-scale 2D monolayer of MoS₂, simultaneously enhancing its optoelectronic properties^[146]. They deposited the monolayer MoS₂ film on a sapphire wafer through the chemical vapor deposition (CVD) method and patterned the channels via dry etching. Under light illumination, the device operates through a photogating effect, where incident light generates electron-hole pairs in the MoS₂ channel. The photogenerated electrons become trapped in localized states within the photoresponsive layer or at defect sites, while the remaining holes contribute

to the channel current, leading to a persistent modulation of conductance. This trapped charge creates a localized electric field that dynamically shifts the threshold voltage, enabling a sustained photoresponse even after the light stimulus is removed. Leveraging the high light absorption coefficient and efficient generation of electron-hole pairs due to the direct bandgap of monolayer MoS₂^[147], the device effectively implemented functions such as visual sensing, memory, and processing under light environments. The MoS₂ vision chip, having successfully performed image preprocessing, represents a novel contribution to the emerging neuromorphic imaging devices. Black phosphorus (bP), another prominent 2D material, is noted for its high hole mobility, considerable anisotropy, robust light-matter interaction, and an extensive spectral range that spans from deep UV to IR wavelengths, making it a versatile candidate in the realm of 2D materials^[148–151]. Lee et al. introduced a multifunctional image sensor built on an array of programmable phototransistors, fabricating black phosphorous programmable phototransistors (bP-PPTs) layers using mechanical exfoliation and a dry transfer method^[152]. The narrow bandgap of bP enables the bP-PPTs to operate as broadband photodetectors capable of detecting NIR light. This relies on charge trapping and field-effect modulation in the gate dielectric stack. Under light illumination, photogenerated electrons in the bP channel are influenced by the gate-induced electric field, leading to electron tunneling into localized states within the HfO₂ layer. The trapped charges effectively shift the threshold voltage and modulate the conductance of the bP channel, enabling dynamic control of the photoresponsivity. This mechanism allows precise adjustment of optical and electrical responses through programmable gate inputs, with the phototransistors retaining their charge states even after the light stimulus is removed, demonstrating non-volatile memory characteristics. Moreover, the bP-PPTs array is employed to vision-sensory functions, allowing for edge detection on images in multiple wavelength bands. An accuracy of 92% was achieved in the MNIST pattern recognition test through the CNNs, indicating the dual functionality in both image processing and recognition tasks.

5.1.2. Oxide-based optoelectronics. Metal oxide semiconductors, which are widely utilized in optoelectronic systems, offer several advantages that make them highly suitable for the development of neuromorphic vision/optoelectronic sensors. Firstly, the layer size and morphology of metal oxide materials can be easily controlled through various synthesis techniques, such as sol-gel process and vacuum deposition methods. Unlike low-dimensional materials, metal oxide materials offer the advantage of large-area fabrication, enabling scalability for industrial applications and large-scale device integration. This scalability allows for the precise tailoring of material characteristics to optimize the performance of optoelectronic devices. The ability to manipulate the nanostructure of these materials directly influences their optical properties, including the band gap and light absorption properties, which are crucial for enhancing the efficiency and sensitivity of optoelectronic components. Secondly, metal oxide materials are known for

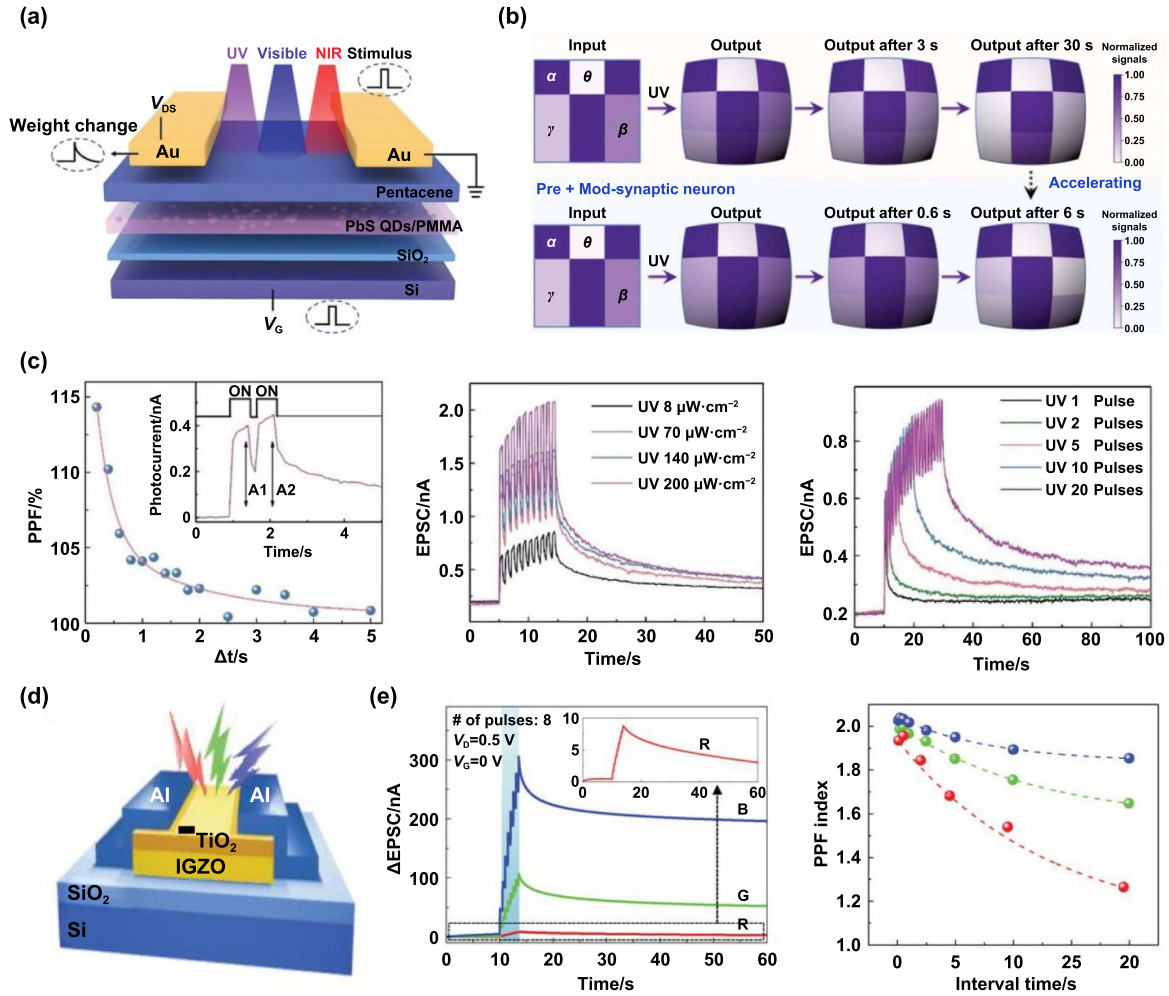


Figure 7. Neuromorphic optoelectronic system with synaptic transistors. (a) Schematic diagram of the broadband optoelectronic synaptic transistor utilizing a PbS QDs/pentacene heterostructure integrated with PbS QDs/poly(methyl methacrylate) photoresponsive charge trapping layer. (b) 3×3 pixelated array subjected to a photonic signal with the wavelength of 365 nm. The contrast enhancement process is demonstrated under the gate-bias of -2 V. (a) and (b)^[124] John Wiley & Sons. © 2023 Wiley-VCH GmbH. (c) Short-term PPF behavior induced by UV light with the wavelength of 390 nm and pulse duration of 500 ms. EPSC response under different UV light pulse numbers and power densities are shown as well.^[126] John Wiley & Sons. © 2023 Wiley-VCH GmbH. (d) Structure of the TiO₂/IGZO heterojunction-based optoelectronic transistor. (e) EPSC response and retention characteristics measured under red, green, and blue visible lights. The last curve shows the variation of PPF index as a function of interval time. (d) and (e)^[127] John Wiley & Sons. © 2023 Wiley-VCH GmbH.

their exceptional stability. This stability is essential in applications where long-term reliability is critical. The chemical and thermal stability of metal oxides ensures that devices maintain high performance over extended periods, thus reducing maintenance costs and improving the overall lifecycle of the technology. Thirdly, the chemical composition of metal oxides is simple and highly adaptable, supporting a variety of technological applications. By doping metal oxides with different elements or integrating them with other materials, it is possible to precisely adjust their electrical, optical, and magnetic properties to suit specific needs.

In this regard, Guo et al. developed a two-terminal optoelectronic synapse using a ZnO/molybdenum trioxide (MoO₃) structure fabricated by the sputtering process^[126]. The device successfully emulates various synaptic functions, including PPF, EPSC (Figure 7(c)). The inherent broadband photo-detective and non-volatile characteristics of ZnO enabled

the sensing of photonic and electronic stimulations and allowed conductance tuning feasible. Also, the MoO₃ served as a hole transport layer that enhances photocurrent generation under light illumination. By controlling the migration of oxygen vacancies, they were able to adjust the barrier height and conductivity of ZnO, enabling the resistive switching. This foundation enabled successful applications in handwritten recognition using neural networks. Additionally, in case of a three-terminal device configuration, a titania (TiO₂)/IGZO heterojunction-based optoelectronic transistor was demonstrated for visible-light-operating neuromorphic applications (Figure 7(d))^[127]. By applying the TiO₂ overlayer on IGZO by sputtering, the light absorption range was extended to include red light, significantly increasing photoresponsivity (Figure 7(e)). The addition of a gate in the three-terminal structure allowed for the regulation of photocarrier dynamics and retention behavior, demonstrating multilevel

conductance states. The employment of metal-oxide materials in optoelectronics offers the significant advantage of being compatible with current available CMOS fabrication techniques. Furthermore, Kwon et al. have introduced an advanced optoelectronic neuromorphic system, integrating a large-area array composed of metal-chalcogenide cadmium sulfide/IGZO heterostructure phototransistors (Figures 8(a)–(c))^[128]. These optoelectronic synaptic device pixel circuits effectively simulate biological synaptic behaviors, such as EPSC and IPSC, to facilitate complex pattern recognition under varying light conditions. The 7×7 neuromorphic pixel circuit array demonstrates the capability of these devices to handle complex pattern recognition through bidirectional synaptic modulation induced by multispectral light. By utilizing wavelength-selective activation of photo-generated charges at the heterostructure interface, the device supports both excitatory and inhibitory synaptic responses. This capability significantly enhances the system's computational tasks, such as image recognition and motion detection, pushing the boundaries of neuromorphic computing within the field of optoelectronics.

5.1.3. Ferroelectric-based optoelectronics. Ferroelectric materials have emerged as key enablers for advanced vision and optoelectronic devices due to their unique combination of electrical and optical properties. Their spontaneous polarization, which can be reversed and retained even after the removal of an external electric field, makes them highly suitable for non-volatile memory and low-power operation^[153]. This property allows ferroelectric materials to store and modulate optical signals efficiently, a critical requirement for artificial vision systems and neuromorphic optoelectronics. Additionally, their high dielectric constants enable strong charge separation and accumulation, enhancing light absorption and charge carrier transport in photodetectors^[154]. Ferroelectric materials also exhibit fast polarization switching, enabling rapid photoresponse and synaptic functionalities essential for real-time image sensing and processing. Furthermore, ferroelectric materials often possess multi-level polarization states and excellent scalability, making them ideal candidates for optoelectronics and neuromorphic vision systems. Their ability to couple electrical and optical properties further can enable multifunctional devices that integrate sensing, processing, and memory functionalities. Cui et al. developed a ferroelectric photosensor network array using a two-terminal heterostructure comprising Pt/Pb($Zr_{0.2}Ti_{0.8}$)O₃ (PZT)/SrRuO₃ (SRO), with PZT serving as the ferroelectric layer and SRO facilitating the epitaxial growth of PZT via pulsed laser deposition^[114]. This device integrates image sensing and processing capabilities, exhibiting multilevel non-volatile photoresponse controlled by the remanent polarization under 365 nm UV light. Utilizing these two-terminal devices as building blocks, the array demonstrated the ability to perform in-sensor Multiply-Accumulate operations and edge detection in images. However, the device only works under UV lights to modulate the ferroelectric polarization to achieve photo-synaptic properties.

To address this issue, a novel structure utilizing a vdW ferroelectric semiconductor transistor (FST) based on α -indium selenide (α -In₂Se₃) has been introduced, exhibiting a nonlinear photoresponse suitable for a retina-like function across a broad wavelength range from deep UV (275 nm) to NIR (808 nm) (Figure 8(d))^[115]. The α -In₂Se₃ layers, mechanically exfoliated using the Scotch tape method, were transferred via a standard wet-transfer technique, employing polypropylene carbonate and polydimethylsiloxane as holders. α -In₂Se₃ can switch to a polarization-up state with a positive gate voltage pulse, while a light pulse induces a polarization-downward shift due to the upward displacement of the middle layer of selenium atoms (Figure 8(e)). To demonstrate the visual adaptation functions, 3×3 array systems were used to dim the images of simple letters, achieving an impressive 93% recognition accuracy by integrating FST-based retinomorphic sensors with FST-based CNNs (Figure 8(f)).

5.1.4. Organic-based optoelectronics. Moreover, organic materials also have become fundamental to the development of optoelectronic systems, owing to their inherent flexibility and mechanical versatility, which distinguish from brittle low-dimensional materials such as graphene or MoS₂, and rigid materials like metal-oxides and ferroelectrics. This flexibility, coupled with their good mechanical properties^[155] and applicability to large-scale solution processing^[156], makes organic materials particularly advantageous for diverse device applications. Organic thin-film transistors (OTFTs), in particular, have emerged as promising candidates for engineering sensory and neuromorphic devices, attributable to their diverse carrier modulation modes^[97,157–160] established photodetection, and adaptation functionalities^[161–163]. However, integrating both photoexcitation and inhibition within a single OTFT poses significant challenges, necessitating a dual approach to charge carrier manipulation within the same channel. Addressing this complexity, He et al. introduced a novel photo-triggered organic active adaptation transistor, featuring dual complementary bulk heterojunctions (BHJs)^[117]. These BHJs consist of a poly{2,2'-(2,5-bis(2-hexyldecyl)-3,6-dioxo-2,3,5,6-tetrahydropyrrolo[3,4-c] pyrrole-1,4-diyl) dithiophene}-5,5'-diyl-alt-thiophen-2,5-diyl} (PDPP3T):[6,6]-phenyl-C61-butyric acid methyl ester (PCBM) BHJ photoresponsive active layer which was fabricated with solution-processing techniques. The two BHJs initiate a photovoltaic effect-induced photoexcitation, as well as dynamic charge trapping-dominated inhibition, which couple together to modulate carrier concentration in the PDPP3T:PCBM channel. Leveraging the inherent flexibility of organic materials, a flexible transistor array was constructed on a PET substrate. Upon light exposure, transient detector responses arise from photoexcitation in the BHJs, while the accumulation of trapped carriers in the dielectric layer shields the gating field, enabling a dynamic inhibition that intensifies under higher light intensities, thereby facilitating active photo-adaptive behavior in a singular device. This breakthrough paves the way for the application of organic neuromorphic visual systems in bioelectronics and robotics.

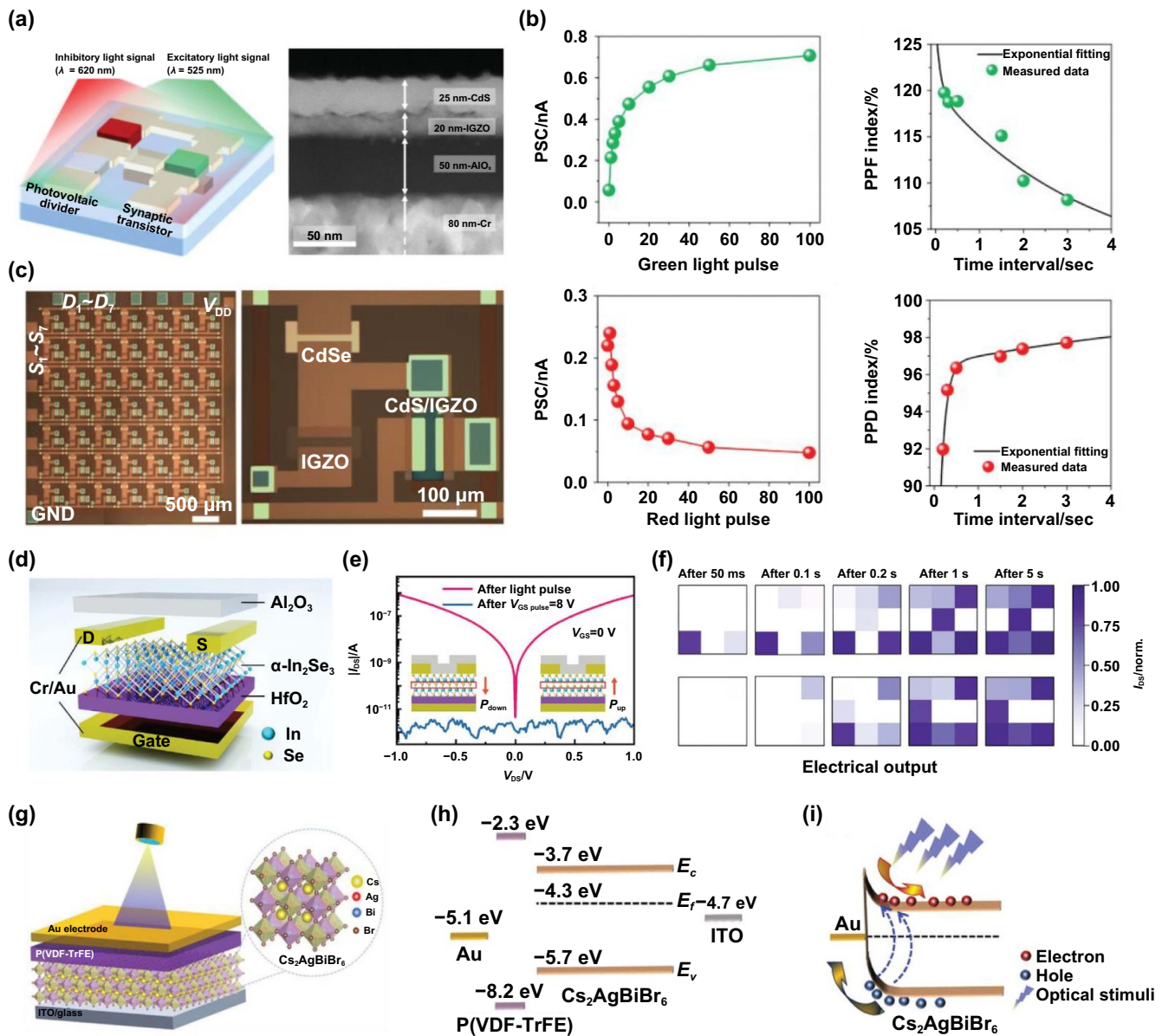


Figure 8. Artificial optoelectronic synapses based on oxide, ferroelectric, perovskite materials. (a) Structure and the cross-sectional scanning transmission electron microscope (STEM) image of the optoelectronic synaptic device (OSD). (b) PSC evolution as the function of 100 green and red light pulses. The PPF index under green light and PPD index under red light was also measured. (c) Photograph and OM images of the 7×7 OSD array. (a)–(c) [128] John Wiley & Sons. © 2021 Wiley-VCH GmbH. (d) Schematic diagram of the FST utilizing α - In_2Se_3 . (e) $V_{\text{DS}}-I_{\text{DSD}}$ curve measured after light pulse and positive gate pulse. The left and right inset depicts the downward and upward polarization states of the α - In_2Se_3 , respectively. (f) Evolution of the optical images of the letter ‘I’ and ‘C’ after illumination under 275 nm deep-ultraviolet light. (d)–(f) [115] John Wiley & Sons. © 2022 Wiley-VCH GmbH. (g) Illustration of the fabricated photonic synapse using $\text{Cs}_2\text{AgBiBr}_6$. (h) The energy band alignment of Au/P(VDF-TrFE)/ $\text{Cs}_2\text{AgBiBr}_6$ /ITO stack. (i) The energy band diagram of Au/ $\text{Cs}_2\text{AgBiBr}_6$ Schottky interface under optical stimuli. (g)–(i) Reproduced from [129]. CC BY 4.0.

5.1.5. Perovskite-based optoelectronics. Perovskite materials have become a leading choice for vision sensors and optoelectronic devices due to their high absorption coefficients, bandgap tunability, and low energy consumption [164]. Their ability to efficiently harvest light in ultra-thin layers makes them highly suitable for broadband photodetectors and compact imaging systems. The bandgap of perovskites

can be precisely tuned through compositional engineering, enabling devices to operate across UV, visible, and NIR wavelengths, which is critical for multispectral imaging and wavelength-specific vision applications. Additionally, their low energy consumption, achieved through efficient photoconductive gain and charge separation at low operating voltages, ensures high performance while minimizing power

requirements. Combined with scalable, low-temperature fabrication methods, these properties position perovskites as a transformative material for advanced optoelectronic and neuromorphic vision systems. Lao et al. showcased an ultralow-power machine vision system utilizing a simple two-terminal self-powered structure comprising Au/P(VDF-TrFE)/Cs₂AgBiBr₆/ITO (Figure 8(g))^[129]. This system featured a strategic band alignment with a potential well at the Schottky energy barrier's shoulder, which significantly prolongs the dwell time of photon-generated carriers within the space-charge region (Figure 8(h)). This arrangement enables the nonlinear interaction of photocurrents induced by spatiotemporal optical signals, a mechanism conclusively verified through polarization-modulated coupling strength between optoelectronic responses (Figure 8(i)). Furthermore, its self-powered operation minimizes external energy requirements, leveraging the photovoltaic characteristics of Cs₂AgBiBr₆ to ensure energy-efficient computation. Moreover, the device demonstrated 99.97% accuracy in classifying face images, achieving this with a training cost vastly lower than that of conventional neural networks, facilitated by photocurrent-encoded in-sensor reservoir computing (RC).

Very recently, Guo et al. spin-coated the mixed halide perovskite Cs_{0.05}MA_{0.15}FA_{0.8}Pb_{0.85}Br_{0.15} to fabricate a heterojunction optoelectronic synapse^[130]. Here, by the ion migration characteristics, the implementation of a stable EPSC depending on the harmonization of the ionic migration barrier was proposed. During the training process, gradual ion accumulation directly influences the learning rate, correlating with the optoelectrical performance of the hardware and allowing for a variable learning rate. This approach markedly enhanced the training speed and achieved a remarkable 97.8% accuracy within just 10 epochs. This investigation demonstrates how controlling the ion migration energy barriers and adjusting readout signals can be potent strategies, laying the groundwork for the development of perovskite devices in advanced photonic neural networks and artificial vision systems.

5.2. Applications of bio-inspired optoelectronic devices

Leveraging insights into the mechanisms of the aforementioned devices, along with advancements in materials and fabrication technologies, numerous optoelectronic devices capable of performing neuromorphic vision functions have been reported. So far, neuromorphic vision systems capable of image adaptation and preprocessing have been developed, which are expected to advance further and contribute to next-generation humanoid robotics and neuromorphic devices. In the following subsection, we summarize recent progress in neuromorphic optoelectronic devices, including visual adaptation^[109,165,166], image processing^[122,167,168], along with their operating mechanisms and distinct optical synaptic functions.

5.2.1. Visual adaptation.

Visual adaptation is a physiological process in which the responsivity of visual organs adjusts to the changes in external brightness, involving both light and dark adaptation^[169,170]. This process includes multiple mechanisms such as the readjustment of optical cells or nerve activity, changes in pupil size, and the transition between photopic and scotopic vision^[171]. Visual adaptation serves to modulate sensitivity, either enhancing it during transitions from strong to weak light or reducing it when moving from dim to bright settings, thereby optimizing human interaction with dynamic environmental conditions^[171]. Emulating such functionality in solid-state devices is thus pivotal for advancing artificial perception systems^[172]. To accomplish the artificial visual adaptation, devices must demonstrate a finely tuned transient response and dynamic adaptation responsive to the intensity of light stimuli. Traditional vision sensors, though capable of detecting such changes, often rely on complex circuits and algorithms that may diminish the efficiency. Therefore, advancing optoelectronic devices that incorporate visual adaptation functionalities and encompass a wide range of perception at the sensory level could significantly improve machine vision capabilities, simplify hardware configurations, and enhance image recognition efficiency. Recently, various reports have demonstrated biomimetic vision sensors with adaptive functions^[109,131,173–175].

Gao et al. introduced a bio-inspired vision sensor employing InP QDs integrated with indium-tin-zinc oxide (ITZO) phototransistors to mimic human visual adaptations (Figure 9(a))^[131]. The device showed significantly enhanced visible light responsivity through the energy band alignment and exceptional gate controllability (Figure 9(b)). By modulating the time-dependent I_{DS} using gate control, the phototransistors could emulate both scotopic and photopic adaptations, influenced by the electroneutrality principle associated with charged oxygen vacancies (Figure 9(c)). This precise control contributed to the emulation of complex synaptic functionalities such as PPF, short-term potentiation, and LTP. This enables adaptive visual capabilities in the phototransistors, showing promising applications in advanced machine vision systems by simplifying the circuitry and reducing the need for complex processing algorithms. Additionally, they demonstrated neural networks using the QDs/ITZO FETs, achieving over 93% accuracy in handwritten pattern recognition. More recently, Wen et al. reported biomimetic artificial nanocluster photoreceptors (ACPs) that emulate the advanced visual functionalities of mantis shrimp eyes^[175]. The device utilized a heterostructure comprising chiral silver nanoclusters and pentacene layers to achieve an all-in-one visual system capable of color vision, adaptive light response, and circular polarization recognition. The silver nanoclusters served as precise charge reservoirs, while the pentacene layer acted as a broadband photodetector, mimicking the multi-receptor arrangement found in biological systems. They further showcased the device's spectral-dependent visual adaptation capabilities, where the photoreceptors responded dynamically

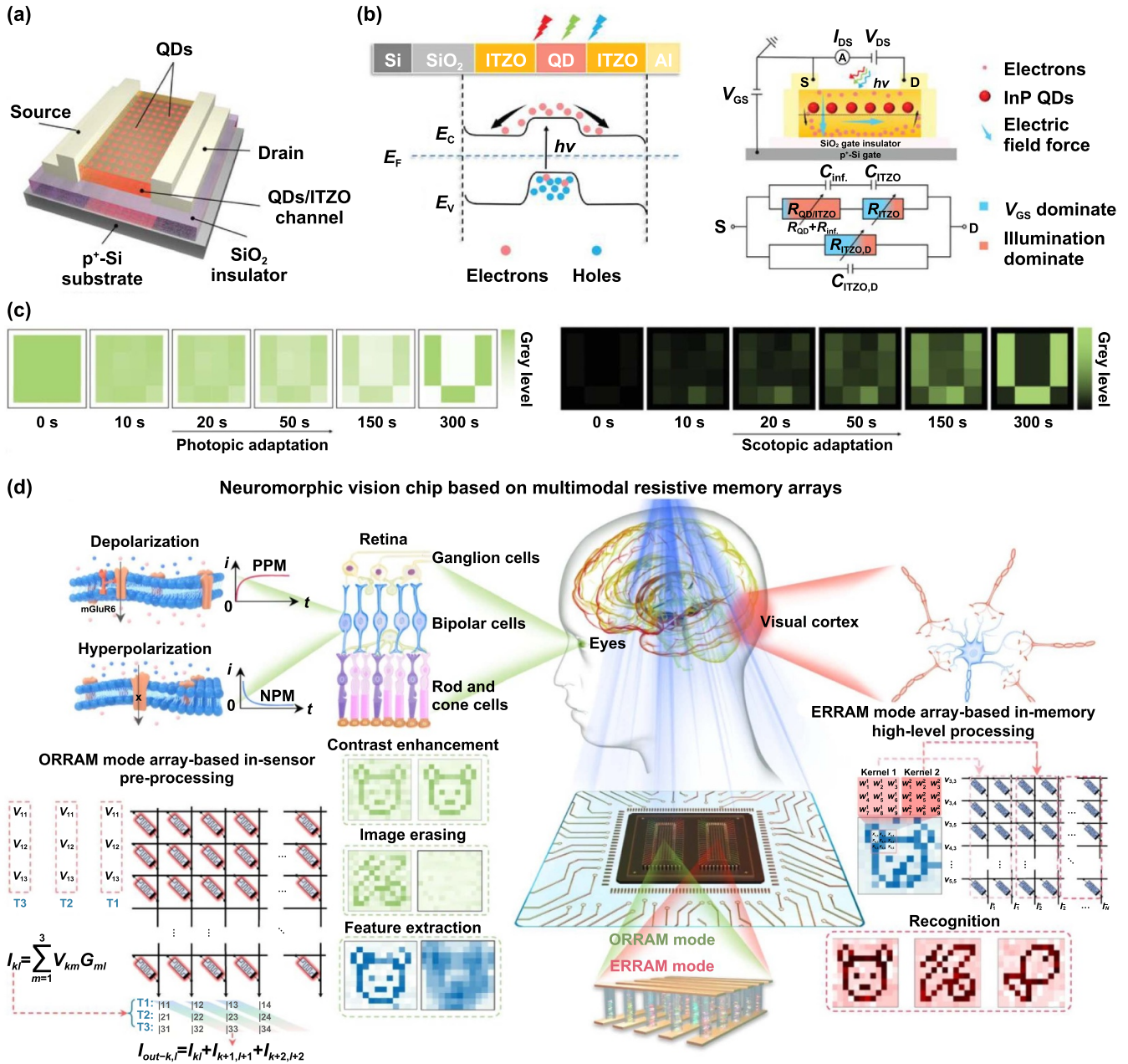


Figure 9. Neuromorphic applications including visual adaptation functions and image processing. (a) Schematic diagram of InP QDs/oxide thin film transistor. (b) The energy band diagram of ITZO/InP QDs/ITZO structure. The carrier transport mechanism and the equivalent circuit model are proposed as well. (c) The evolution of the pattern ‘V’ as a function of time under photopic adaptation and scotopic adaption conditions. (a)–(c)^[131] John Wiley & Sons. © 2023 Wiley-VCH GmbH. (d) Illustration of neuromorphic vision chip based on multimodal resistive memory arrays. The proposed system can be operated in two modes: ORRAM and ERRAM. ORRAM mode is capable of image pre-processing, and ERRAM mode can achieve high-level image recognition, indicating high versatility of the neuromorphic visual system. Reproduced from^[133]. CC BY 4.0.

to light of varying intensities and wavelengths. This adaptation was achieved through a synergistic interaction between gate voltage and light stimuli, with the charge trapping and release dynamics in the nanoclusters playing a pivotal role. The ACPs exhibited rapid adaptation times and a wide perception range, highlighting their potential for real-time image adaptation in diverse lighting conditions. These results demonstrate the potential of visual adaptation application in bridging

the gap between biological and artificial vision, offering a pathway toward next-generation neuromorphic and optoelectronic devices.

5.2.2. Neuromorphic image processing. In the field of optoelectronics, the application of contrast enhancement^[108,176–178] and noise reduction^[179–181] are critical for enhancing the quality and functionality of imaging

systems. Contrast enhancement applications are essential for improving the visibility of features in an image by increasing the difference in luminance or color, making it easier to distinguish objects from the background. In addition to contrast enhancement, noise reduction is also crucial for eliminating undesirable artifacts from images, which may arise from environmental factors, or during image capture and transmission. Effective noise reduction ensures clear and precise images, essential in autonomous and robot visions. These applications enhance image clarity and detail, while simultaneously elevating the efficiency of subsequent image processing operations, driving forward technological innovations in optoelectronic systems.

Contrast enhancement and noise reduction in artificial vision systems can be achieved using optoelectronic synaptic transistors that integrate InP/ZnSe QDs with SnO₂^[132]. These devices utilize the photoresponsive properties of QDs to modulate the electrical conductance in response to light intensity changes. The light-induced charge carriers increase the conductance of SnO₂ channel, directly improving the contrast and image denoising in visual signals. This significantly enhances image clarity and assists in streamlining the computational efforts needed for subsequent neural network processing.

More recently, Zhou et al. demonstrated a full hardware implementation of a neuromorphic visual system utilizing multimodal optoelectronic resistive memory arrays for comprehensive image processing functions (Figure 9(d))^[133]. This system, based on modified silk fibroin protein, includes both optoelectronic and electrical resistive random-access memory modes. These modes facilitated advanced image preprocessing capabilities directly on the sensor hardware, significantly simplifying circuit design and reducing the complexity of fabrication and integration. Specifically, the system employed optoelectronic resistive random access memory mode for in-sensor image preprocessing tasks such as contrast enhancement, background denoising, feature extraction, and electrical resistive random access memory mode for near-sensor high-level image recognition. This setup enhances integration density while closely aligning with neuromorphic processing principles, showcasing the potential for a leap towards efficient, high-density, and low-power sensory computing.

5.3. Bio-inspired optoelectronic devices using artificial neural networks

In addition to mimicking the preprocessing function of human retina, the optoelectronic devices have the ability to trigger multi-level and non-volatile memory, which is very significant for simulating the synaptic connection of the visual cortex and achieving the image recognition function^[182–184]. ANNs, one of the pivotal ML algorithms, utilize feedforward and backpropagation mechanisms for weight updates to facilitate learning^[185]. This capability has made the ANNs a focal point in numerous fields, particularly in AI applications such as

image recognition^[186–188]. Non-volatile photosensors leverage their ability to possess different weights, enabling parallel processing that is extensively applied across various applications. However, ANNs often struggle to identify optimal parameters during training and are known for their relatively slow learning speeds, highlighting the need for alternative neural network training algorithms.

CNNs which utilize multiple convolutional kernels to extract and learn features from images, show outstanding performance in image and video analysis due to their unique characteristics^[189]. Compared to traditionally fully connected feedforward networks, CNNs require fewer parameters, lower training costs, and better recognition rates, making them well-suited for optoelectronic applications such as image recognition and motion detection^[134,138,190,191]. Zhu et al. demonstrated optoelectronic synapses based on 2D molecular crystal heterojunctions that directly modulate synaptic weights in response to light, which plays a critical role in enhancing CNN-based image recognition (Figure 10(a))^[134]. The synapses showed EPSC and IPSC, adapting dynamically to visual inputs based on light intensity and gate voltage control (Figures 10(b)–(d)). Real-time synaptic adjustment enables the CNN to process images more efficiently by reducing the need for computationally intensive training (Figure 10(e)). The bidirectional synaptic behavior, triggered by optical stimuli, significantly improves the performance in motion detection tasks, making the system highly effective for image recognition with fast response times and lower power consumption.

Another neural network algorithm, RC, is based on non-linearity and projects input data into a high-dimensional space through a reservoir layer^[192]. This approach significantly simplifies training by only requiring updates to the weights at the output layer, thereby reducing learning complexity and time^[193]. Consequently, RC enables ultra-high speed and ultra-low power consumption, presenting substantial advantages over other algorithms. More recently, Wu et al. employ in-sensor RC with optoelectronic synaptic transistors, ingeniously constructed by covalently bonding cations and anions with a flexible alkyl chain^[135]. This unique design effectively prevented the long-range migration of free ions during polarization and ensured consistent polarization-relaxation dynamics under various presynaptic inputs. As a result, the system achieved low operation voltage and minimal power consumption. Moreover, the transistors exhibited a diverse of optoelectrical synaptic behaviors, such as EPSC, PPF, STP, LTP, short-term memory (STM), and long-term memory (LTM). These capabilities render the device exceptionally effective for tasks such as image sensing, data memorization, and real-time preprocessing. Demonstrating the practical application of the technology, the device excels in high-performance motion tracking, accurately capturing the movement of basketballs with a precision rate of 95.56%, enhancing motion detection capabilities and setting a new standard for integrating sensory and processing functions in optoelectronic devices.

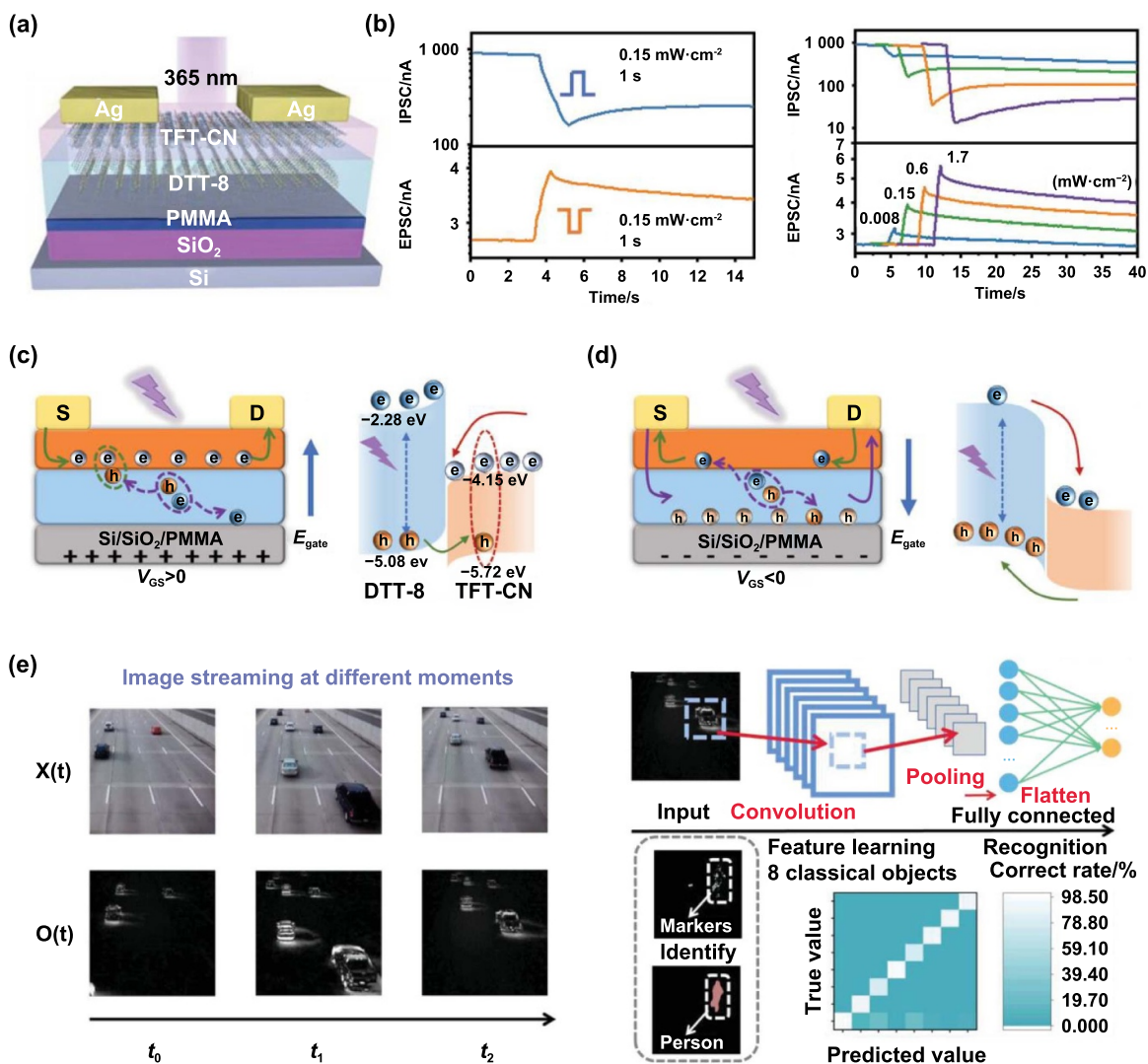


Figure 10. Artificial visual systems integrated with ANNs. (a) Device structure of a synaptic transistor with 2D molecular crystal p-n heterojunction. (b) EPSC and IPSC variation of the synaptic transistor with varying light intensities. (c) Working principles of the transistor in the case of positive gate-bias. (d) Working principles of the transistor in the case of negative gate-bias. (e) Applications utilizing ANNs. Motion of the moving vehicles was detected at different moments. Further, with the aid of already trained CNN, 8 types of tagged objects were identified with a recognition rate exceeding 90%.^[134] John Wiley & Sons. © 2023 Wiley-VCH GmbH.

6. Summary and outlook

Recent advancements in bio-inspired neuromorphic sensory devices have considerably advanced the integration and performance of systems that emulate human senses such as tactility, audition, olfaction, gustation, and vision. These systems employ a diverse array of materials to replicate the complexities of human sensory inputs in robotics and autonomous systems. Here, we have extensively reviewed the progress of artificial sensory devices from perspectives of materials, fabrication processes, device structure, synaptic functions, system integration methods, and neuromorphic applications. To overcome the limitations of conventional material-based sensors, emerging materials such as MXene, liquid metals, ionic gel, ferroelectric materials, and perovskites were employed for neuromorphic sensors, utilizing their unique advantages. With the various materials, sensors and artificial synaptic devices

with two- and three-terminal structures have been fabricated by combining vacuum-based processes and other fabrication methods. The fabricated sensors and synaptic devices were either monolithically or heterogeneously integrated, demonstrating diverse neuromorphic applications.

Despite these innovations, several challenges persist that could hinder their wider application and effectiveness (Figure 11). Firstly, the integration of various materials such as organics, inorganics, and polymers, while still in its early stages, often leads to a poor understanding of growth conditions and modifications, resulting in physical properties and interface incompatibilities. These issues could degrade the efficiency and durability of sensory devices, leading to problems with sensory accuracy. Consequently, neuromorphic sensory systems could improve interface engineering through enhanced molecular-level control. Employing self-assembling materials or developing new composite

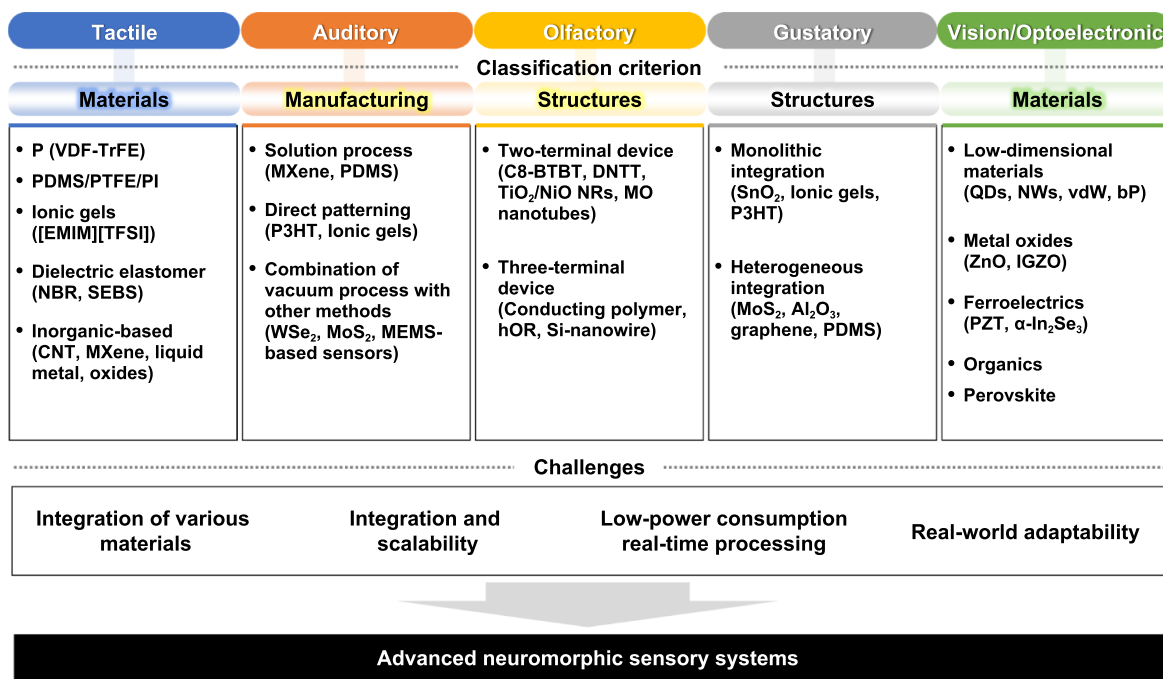


Figure 11. Classification of criteria and future challenges for neuromorphic sensory devices.

materials that inherently blend the properties of organics and inorganics might facilitate seamless integration, thereby enhancing device performance and longevity. Secondly, research must advance in terms of integration and scalability. Integrating sensory systems into a cohesive unit capable of mimicking human sensory processing remains complex and costly. Many current designs optimize individual sensory modalities without considering their integration into larger systems. Moreover, scaling these technologies from laboratory prototypes to commercially viable products poses significant technical and economic challenges, including maintaining the performance at larger scales and ensuring consistency and reliability across manufacturing batches. Specifically, a variety of emerging materials are expected to encounter challenges in large-area mass production, which can enlarge the gap between academia and industry. A majority of 2D materials in particular, are fabricated via exfoliation or solution-based processes, resulting in difficult patterning process and large-area device fabrication. Although CVD processes are currently being employed for the deposition of 2D materials, there are still scalability and integration challenges to be overcome. Atomic and close-to-atomic scale manufacturing (ACSM) can be a viable alternative for ensuring the mass production. ACSM methods, including site-selective CVD, area-selective ALD, electrodeposition, and laser-assisted synthesis can possibly enable high CMOS process compatibility along with uniform large-area fabrication^[194]. Achieving mass production while reducing the production cost is also crucial to successful commercialization. Laser-induced forward transfer (LIFT) method can be considered as a possible way for cost reduction^[195]. The LIFT method is a nozzle-free, pixel-by-pixel direct writing technique, without the need for additional masks, screens, or rolls, thereby simplifying the

fabrication process while maintaining high quality. Also, it is able to print a wide range of materials, and can achieve high-resolution patterning along with fast fabrication speed, compared to conventional fabrication methods. Thirdly, enhancements are needed in low-power consumption and real-time processing. Neuromorphic devices typically require substantial power for continuous data processing and response generation. Reducing power consumption while maintaining or enhancing processing speeds is crucial, particularly for portable and implantable devices. Advanced computational models and materials that allow for lower power consumption and faster data processing are essential to address these challenges. Most importantly, real-world adaptability is crucial. While laboratory results are promising, translating these findings to real-world applications presents significant challenges. This includes ensuring the effective operation of devices against diverse and unpredictable environmental conditions, apart from controlled laboratory environment. Developing adaptive algorithms and robust designs that can handle real-world variability and complexity is necessary to advance the practical deployment of these technologies.

Looking ahead, the field of bio-inspired neuromorphic sensory devices stands at a critical juncture. This is an interdisciplinary field where various disciplines must bring their own unique insight and expertise for the advancement in neuromorphic sensory system technology. Future research should focus on overcoming these challenges through interdisciplinary collaboration, leveraging advances in neuroscience, materials science, computer engineering, and robotics. Here in this review, we propose several future research directions mainly focused on interdisciplinary collaboration, related to the above-mentioned challenges.

First of all, contribution from neuroscientists is required, since deeper knowledge of neuroscience can promote the understanding of sensing mechanisms and ANNs. For this, neurobiologists should collaborate with various engineers, bridging the gap between real biological systems and artificial systems. Specifically, neurobiologists can suggest biological models from various organisms, providing insight for the development of advanced neuromorphic sensing systems and algorithms. Further understanding of how the human brain adapts and reacts to environmental changes can also facilitate the development of monolithically integrated real-time sensors. Second, interdisciplinary research direction for neuromorphic sensory systems requires assistance from computer engineering field. Although few integrated sensory systems have demonstrated real-time sensing and processing of sensory information^[196], the biggest challenge AI model encounters is still the real-world scenario. Numerous sensory system reports have acquired high network performance on trained and limited data, but failed to demonstrate how the system can process real-time obtained new data. To overcome this challenge, computer engineers should create ML techniques and algorithms to better react to untrained data. Recently, few works on adaptive algorithms have been reported from various fields^[197–200], suggesting the pathway that ML algorithms should evolve towards. Another important research direction includes collaboration with neurorobotics field. For the development of humanoid robots and prosthetics, neuromorphic sensors must be integrated with neurobotic technology. Biocompatibility and interface communication issues must be addressed, and further development of brain-machine interfaces is required. Research should also focus on improving the response time of sensors and the robot's speed of neural signal processing. For better real-time interaction of robots with their surroundings, computer engineers must improve deep learning techniques^[201] and suggest new types of robotic algorithms for social and swarm intelligence^[202,203]. Above all, material scientists and physicists must continuously excavate new sensing materials and semiconductors with high stability. Further collaboration with various engineers must be carried out as well, to ensure the large-area fabrication capability of emerging materials.

Acknowledgment

This work was supported by the National Research Foundation of Korea (NRF) Grant funded by the Korea Government (Ministry of Science and ICT) (No. NRF-2022R1A2C2010774), by the GRRC program of Gyeonggi Province (GRRC Sungkyunkwan 2023-B04), and by Korea Institute for Advancement of Technology (KIAT) grant funded by the Korea Government (MOTIE) (P0020967, Advanced Training Program for Smart Sensor Engineers).

ORCID iD

Yong-Hoon Kim  <https://orcid.org/0000-0003-0057-1893>

References

- [1] Cai P Q et al. 2020. Locally coupled electromechanical interfaces based on cytoadhesion-inspired hybrids to identify muscular excitation-contraction signatures. *Nat. Commun.* **11**, 2183.
- [2] Guo H Y et al. 2018. A highly sensitive, self-powered triboelectric auditory sensor for social robotics and hearing aids. *Sci. Robot.* **3**, eaat2516.
- [3] Jung Y H, Park B, Kim J U and Kim T-I. 2019. Bioinspired electronics for artificial sensory systems. *Adv. Mater.* **31**, 1803637.
- [4] He K, Wang C, He Y L, Su J T and Chen X D. 2023. Artificial neuron devices. *Chem. Rev.* **123**, 13796–13865.
- [5] Sun F Q, Lu Q F, Feng S M and Zhang T. 2021. Flexible artificial sensory systems based on neuromorphic devices. *ACS Nano* **15**, 3875–3899.
- [6] Tian H, Zhao L F, Wang X F, Yeh Y-W, Yao N, Rand B P and Ren T-L. 2017. Extremely low operating current resistive memory based on exfoliated 2D perovskite single crystals for neuromorphic computing. *ACS Nano* **11**, 12247–12256.
- [7] Zhang C et al. 2019. Bioinspired artificial sensory nerve based on nafion memristor. *Adv. Funct. Mater.* **29**, 1808783.
- [8] Hu L X, Fu S, Chen Y H, Cao H T, Liang L Y, Zhang H L, Gao J H, Wang J R and Zhuge F. 2017. Ultrasensitive memristive synapses based on lightly oxidized sulfide films. *Adv. Mater.* **29**, 1606927.
- [9] Tan Z-H, Yang R, Terabe K, Yin X-B, Zhang X-D and Guo X. 2016. Synaptic metaplasticity realized in oxide memristive devices. *Adv. Mater.* **28**, 377–384.
- [10] Gkoupidenis P, Schaefer N, Strakosas X, Fairfield J A and Malliaras G G. 2015. Synaptic plasticity functions in an organic electrochemical transistor. *Appl. Phys. Lett.* **107**, 263302.
- [11] Yan X D, Qian J H, Sangwan V K and Hersam M C. 2022. Progress and challenges for memtransistors in neuromorphic circuits and systems. *Adv. Mater.* **34**, 2108025.
- [12] Chen L et al. 2024. Bioinspired iontronic synapse fibers for ultralow-power multiplexing neuromorphic sensorimotor textiles. *Proc. Natl Acad. Sci. USA* **121**, e2407971121.
- [13] Li Y, Qiu Z C, Kan H, Yang Y, Liu J W, Liu Z R, Yue W J, Du G Q, Wang C and Kim N-Y. 2024. A human-computer interaction strategy for an FPGA platform boosted integrated “perception-memory” system based on electronic tattoos and memristors. *Adv. Sci.* **11**, 2402582.
- [14] Li Y, Lin Q H, Sun T, Qin M Z, Yue W J and Gao S. 2024. A perceptual and interactive integration strategy toward telemedicine healthcare based on electroluminescent display and triboelectric sensing 3D stacked device. *Adv. Funct. Mater.* **34**, 2402356.
- [15] Yang W H, Kan H, Shen G Z and Li Y. 2024. A network intrusion detection system with broadband $\text{WO}_{3-x}/\text{WO}_{3-x}-\text{Ag}/\text{WO}_{3-x}$ optoelectronic memristor. *Adv. Funct. Mater.* **34**, 2312885.
- [16] Wang W S and Zhu L Q. 2023. Recent advances in neuromorphic transistors for artificial perception applications. *Sci. Technol. Adv. Mater.* **24**, 2152290.
- [17] Yu J R, Wang Y F, Qin S S, Gao G Y, Xu C, Wang Z L and Sun Q J. 2022. Bioinspired interactive neuromorphic devices. *Mater. Today* **60**, 158–182.
- [18] Huynh H Q, Trung T Q, Bag A, Do T D, Sultan M J, Kim M and Lee N-E. 2023. Bio-inspired artificial fast-adaptive and slow-adaptive mechanoreceptors with synapse-like functions. *Adv. Funct. Mater.* **33**, 2303535.
- [19] Zhang T, Zhao M H, Zhai M X, Wang L S, Ma X Y, Liao S M, Wang X N, Liu Y J and Chen D. 2024. Improving the resolution of flexible large-area tactile sensors through machine-learning perception. *ACS Appl. Mater. Interfaces* **16**, 11013–11025.

- [20] Niu H S, Li H, Gao S, Li Y, Wei X, Chen Y K, Yue W J, Zhou W J and Shen G Z. 2022. Perception-to-cognition tactile sensing based on artificial-intelligence-motivated human full-skin bionic electronic skin. *Adv. Mater.* **34**, 2202622.
- [21] Han J-K, Tcho I-W, Jeon S-B, Yu J-M, Kim W-G and Choi Y-K. 2022. Self-powered artificial mechanoreceptor based on triboelectrification for a neuromorphic tactile system. *Adv. Sci.* **9**, 2105076.
- [22] Tan H W, Tao Q Z, Pande I, Majumdar S, Liu F, Zhou Y F, Persson P O Å, Rosen J and van Dijken S. 2020. Tactile sensory coding and learning with bio-inspired optoelectronic spiking afferent nerves. *Nat. Commun.* **11**, 1369.
- [23] Kweon H et al. 2023. Ion trap and release dynamics enables noninvasive tactile augmentation in monolithic sensory neuron. *Sci. Adv.* **9**, eadi3827.
- [24] Seo S et al. 2020. Artificial van der Waals hybrid synapse and its application to acoustic pattern recognition. *Nat. Commun.* **11**, 3936.
- [25] Bolat S et al. 2020. Synaptic transistors with aluminum oxide dielectrics enabling full audio frequency range signal processing. *Sci. Rep.* **10**, 16664.
- [26] Gou G-Y et al. 2022. Two-stage amplification of an ultrasensitive MXene-based intelligent artificial eardrum. *Sci. Adv.* **8**, eabn2156.
- [27] Yun S-Y, Han J-K, Lee S-W, Yu J-M, Jeon S-B and Choi Y-K. 2023. Self-aware artificial auditory neuron with a triboelectric sensor for spike-based neuromorphic hardware. *Nano Energy* **109**, 108322.
- [28] Zhang J Y, Dai S L, Zhao Y W, Zhang J H and Huang J. 2020. Recent progress in photonic synapses for neuromorphic systems. *Adv. Intell. Syst.* **2**, 1900136.
- [29] Lee Y and Lee T-W. 2019. Organic synapses for neuromorphic electronics: from brain-inspired computing to sensorimotor nervertronics. *Acc. Chem. Res.* **52**, 964–974.
- [30] Ohigashi H, Koga K, Suzuki M, Nakanishi T, Kimura K and Hashimoto N. 1984. Piezoelectric and ferroelectric properties of P (VDF-TrFE) copolymers and their application to ultrasonic transducers. *Ferroelectrics* **60**, 263–276.
- [31] Kim H, Oh S, Choo H, Kang D H and Park J H. 2023. Tactile neuromorphic system: convergence of triboelectric polymer sensor and ferroelectric polymer synapse. *ACS Nano* **17**, 17332–17341.
- [32] Cho J H, Lee J, Xia Y, Kim B, He Y Y, Renn M J, Lodge T P and Daniel Frisbie C. 2008. Printable ion-gel gate dielectrics for low-voltage polymer thin-film transistors on plastic. *Nat. Mater.* **7**, 900–906.
- [33] Gao N W and Pan C F. 2024. Intelligent ion gels: design, performance, and applications. *SmartMat* **5**, e1215.
- [34] Wang B H, Huang W, Chi L F, Al-Hashimi M, Marks T J and Facchetti A. 2018. High-*k* gate dielectrics for emerging flexible and stretchable electronics. *Chem. Rev.* **118**, 5690–5754.
- [35] Jonscher A K. 1999. Dielectric relaxation in solids. *J. Phys. D: Appl. Phys.* **32**, R57–R70.
- [36] Wang W C et al. 2023. Neuromorphic sensorimotor loop embodied by monolithically integrated, low-voltage, soft e-skin. *Science* **380**, 735–742.
- [37] Ham S, Kang M J, Jang S, Jang J, Choi S, Kim T-W and Wang G. 2020. One-dimensional organic artificial multi-synapses enabling electronic textile neural network for wearable neuromorphic applications. *Sci. Adv.* **6**, eaba1178.
- [38] Wang S R, Kang Y F, Wang L W, Zhang H X, Wang Y S and Wang Y. 2013. Organic/inorganic hybrid sensors: a review. *Sens. Actuators B* **182**, 467–481.
- [39] Eivazzadeh-Keihan R et al. 2022. Applications of carbon-based conductive nanomaterials in biosensors. *Chem. Eng. J.* **442**, 136183.
- [40] Chun S, Son W, Kim H, Lim S K, Pang C and Choi C. 2019. Self-powered pressure- and vibration-sensitive tactile sensors for learning technique-based neural finger skin. *Nano Lett.* **19**, 3305–3312.
- [41] Kim S, Lee Y, Kim H D and Choi S J. 2020. A tactile sensor system with sensory neurons and a perceptual synaptic network based on semivolatiles carbon nanotube transistors. *NPG Asia Mater.* **12**, 76.
- [42] Li Y et al. 2022. Multifunctional biomimetic tactile system via a stick-slip sensing strategy for human-machine interactions. *npj Flex. Electron.* **6**, 46.
- [43] Vu C C and Kim J. 2018. Human motion recognition by textile sensors based on machine learning algorithms. *Sensors* **18**, 3109.
- [44] Vu C C and Kim J. 2020. Highly elastic capacitive pressure sensor based on smart textiles for full-range human motion monitoring. *Sens. Actuators A* **314**, 112029.
- [45] Wen F, Sun Z D, He T Y Y, Shi Q F, Zhu M L, Zhang Z X, Li L H, Zhang T and Lee C. 2020. Machine learning glove using self-powered conductive superhydrophobic triboelectric textile for gesture recognition in VR/AR applications. *Adv. Sci.* **7**, 2000261.
- [46] Ho D H, Choi Y Y, Jo S B, Myoung J-M and Cho J H. 2021. Sensing with MXenes: progress and prospects. *Adv. Mater.* **33**, 2005846.
- [47] Pei Y Y, Zhang X L, Hui Z Y, Zhou J Y, Huang X, Sun G Z and Huang W. 2021. Ti₃C₂T_xMXene for sensing applications: recent progress, design principles, and future perspectives. *ACS Nano* **15**, 3996–4017.
- [48] Xie X K et al. 2024. Neuromorphic computing-assisted triboelectric capacitive-coupled tactile sensor array for wireless mixed reality interaction. *ACS Nano* **18**, 17041–17052.
- [49] Gao F-L, Liu J, Li X-P, Ma Q, Zhang T T, Yu Z-Z, Shang J, Li R-W and Li X F. 2023. Ti₃C₂T_x MXene-based multifunctional tactile sensors for precisely detecting and distinguishing temperature and pressure stimuli. *ACS Nano* **17**, 16036–16047.
- [50] Zhang S C, Xiao Y, Chen H M, Zhang Y L, Liu H Y, Qu C M, Shao H X and Xu Y. 2023. Flexible triboelectric tactile sensor based on a robust MXene/leather film for human-machine interaction. *ACS Appl. Mater. Interfaces* **15**, 13802–13812.
- [51] Huang J H et al. 2024. A bioinspired MXene-based flexible sensory neuron for tactile near-sensor computing. *Nano Energy* **126**, 109684.
- [52] Kaneko T, Wang Y-F, Hori M, Sekine T, Yoshida A, Takeda Y, Kumaki D and Tokito S. 2023. Printed bilayer liquid metal soft sensors for strain and tactile perception in soft robotics. *Adv. Mater. Technol.* **8**, 2300436.
- [53] Li N, Yuan X H, Li Y Q, Zhang G C, Yang Q H, Zhou Y X, Guo M H and Liu J. 2024. Bioinspired liquid metal based soft humanoid robots. *Adv. Mater.* **36**, 2404330.
- [54] Wang Z H, Lei K C, Tang H Z, Luo Y, Zhao H F, He P S, Ding W B and Lin L W. 2024. Stretchable liquid metal E-skin for soft robot proprioceptive vibration sensing. *IEEE Sens. J.* **24**, 18327–18335.
- [55] Kim H, Zan G T, Seo Y, Lee S and Park C. 2024. Stimuli-responsive liquid metal hybrids for human-interactive electronics. *Adv. Funct. Mater.* **34**, 2308703.
- [56] Li Y Z et al. 2024. A palm-like 3D tactile sensor based on liquid-metal triboelectric nanogenerator for underwater robot gripper. *Nano Res.* **17**, 10008–10016.
- [57] Guthrie R and Isac M. 2012. *In-situ* sensors for liquid metal quality. *High Temp. Mater. Process.* **31**, 633–643.
- [58] Mokhtari M, Wada T, Le Bourlot C, Duchet-Rumeau J, Kato H, Maire E and Mary N. 2020. Corrosion resistance of porous ferritic stainless steel produced by liquid metal dealloying of Incoloy 800. *Corros. Sci.* **166**, 108468.

- [59] Kumar M, Singh R, Kang H, Kim S and Seo H. 2020. An artificial piezotronic synapse for tactile perception. *Nano Energy* **73**, 104756.
- [60] Hajara P, Shijeesh M R, Rose T P and Saji K J. 2024. ZnO-based triboelectric nanogenerator and tribotronic transistor for tactile switch and displacement sensor applications. *Sens. Actuators A* **377**, 115728.
- [61] Gao W X, Zhu Y, Wang Y J, Yuan G L and Liu J-M. 2020. A review of flexible perovskite oxide ferroelectric films and their application. *J. Mater.* **6**, 1–16.
- [62] Drake R L, Vogl A W and Mitchell A W M. 2009. *Gray's Anatomy for Students*. 2nd edn (Elsevier) pp 902–903.
- [63] Su T Y, Liu N S, Lei D D, Wang L X, Ren Z Q, Zhang Q X, Su J, Zhang Z and Gao Y H. 2022. Flexible MXene/bacterial cellulose film sound detector based on piezoresistive sensing mechanism. *ACS Nano* **16**, 8461–8471.
- [64] Gong S, Yap L W, Zhu Y, Zhu B W, Wang Y, Ling Y Z, Zhao Y M, An T C, Lu Y R and Cheng W L. 2020. A soft resistive acoustic sensor based on suspended standing nanowire membranes with point crack design. *Adv. Funct. Mater.* **30**, 1910717.
- [65] Jung Y H, Pham T X, Issa D, Wang H S, Lee J H, Chung M, Lee B-Y, Kim G, Yoo C D and Lee K J. 2022. Deep learning-based noise robust flexible piezoelectric acoustic sensors for speech processing. *Nano Energy* **101**, 107610.
- [66] Chen J W, Li L L, Ran W H, Chen D, Wang L L and Shen G Z. 2023. An intelligent MXene/MoS₂ acoustic sensor with high accuracy for mechano-acoustic recognition. *Nano Res.* **16**, 3180–3187.
- [67] Seo D-G et al. 2019. Versatile neuromorphic electronics by modulating synaptic decay of single organic synaptic transistor: from artificial neural networks to neuro-prosthetics. *Nano Energy* **65**, 104035.
- [68] Huang Q J and Zhu Y. 2019. Printing conductive nanomaterials for flexible and stretchable electronics: a review of materials, processes, and applications. *Adv. Mater. Technol.* **4**, 1800546.
- [69] Goldoni R, Ozkan-Aydin Y, Kim Y-S, Kim J, Zavanelli N, Mahmood M, Liu B Y, Hammond F L III, Goldman D I and Yeo W-H. 2020. Stretchable nanocomposite sensors, nanomembrane interconnectors, and wireless electronics toward feedback-loop control of a soft earthworm robot. *ACS Appl. Mater. Interfaces* **12**, 43388–43397.
- [70] Xu Y C, Deng Z H, Jin C X, Liu W R, Shi X F, Chang J H, Yu H R, Liu B, Sun J and Yang J L. 2023. An organic electrochemical synaptic transistor array for neuromorphic computation of sound localization. *Appl. Phys. Lett.* **123**, 133701.
- [71] Wu X L, Dang B J, Wang H, Wu X L and Yang Y C. 2022. Spike-enabled audio learning in multilevel synaptic memristor array-based spiking neural network. *Adv. Intell. Syst.* **4**, 2100151.
- [72] İlik B, Koyuncuoğlu A, Şardan-Sukas Ö and Külah H. 2018. Thin film piezoelectric acoustic transducer for fully implantable cochlear implants. *Sens. Actuators A* **280**, 38–46.
- [73] Wang W, Pedretti G, Milo V, Carboni R, Calderoni A, Ramaswamy N, Spinelli A S and Ielmini D. 2018. Learning of spatiotemporal patterns in a spiking neural network with resistive switching synapses. *Sci. Adv.* **4**, eaat4752.
- [74] Zhou C Z, Zang J B, Xue C Y, Ma Y X, Hua X Q, Gao R, Zhang Z X, Li B and Zhang Z D. 2022. Design of a novel medical acoustic sensor based on MEMS bionic fish ear structure. *Micromachines* **13**, 163.
- [75] Moro F et al. 2022. Neuromorphic object localization using resistive memories and ultrasonic transducers. *Nat. Commun.* **13**, 3506.
- [76] Das S, Dodda A and Das S. 2019. A biomimetic 2D transistor for audiomorphic computing. *Nat. Commun.* **10**, 3450.
- [77] Oh S, Lee J-H, Seo S, Choo H, Lee D, Cho J-I and Park J-H. 2022. Electrolyte-gated vertical synapse array based on van der Waals heterostructure for parallel computing. *Adv. Sci.* **9**, 2103808.
- [78] Seo S et al. 2018. Artificial optic-neural synapse for colored and color-mixed pattern recognition. *Nat. Commun.* **9**, 5106.
- [79] Lenk C et al. 2023. Neuromorphic acoustic sensing using an adaptive microelectromechanical cochlea with integrated feedback. *Nat. Electron.* **6**, 370–380.
- [80] Lenk C, Ivanov T, Durstewitz S, Ved K, Gubbi V and Ziegler M. 2023. An adaptive acoustic neuromorphic auditory system. In *Proc. 2023 IEEE Nanotechnology Materials and Devices Conference* (IEEE) pp 210–211.
- [81] Hajare R, Reddy V and Srikanth R. 2022. MEMS based sensors—a comprehensive review of commonly used fabrication techniques. *Mater. Today Proc.* **49**, 720–730.
- [82] Taylor M R, Simon E J, Dickey J L, Hogan K A and Reece J B. 2017. *Campbell Biology: Concepts & Connections*. 9th edn (Pearson) pp 603.
- [83] Chun S Y, Song Y G, Kim J E, Kwon J U, Soh K, Kwon J Y, Kang C-Y and Yoon J H. 2023. An artificial olfactory system based on a chemi-memristive device. *Adv. Mater.* **35**, 2302219.
- [84] Deng Y P et al. 2023. A flexible and biomimetic olfactory synapse with gasotransmitter-mediated plasticity. *Adv. Funct. Mater.* **33**, 2214139.
- [85] Song H W, Moon D, Won Y, Cha Y K, Yoo J, Park T H and Oh J H. 2024. A pattern recognition artificial olfactory system based on human olfactory receptors and organic synaptic devices. *Sci. Adv.* **10**, ead12882.
- [86] Lee S-W, Kang M, Han J-K, Yun S-Y, Park I and Choi Y-K. 2023. An artificial olfactory sensory neuron for selective gas detection with in-sensor computing. *Device* **1**, 100063.
- [87] Chu Y J, Tan H T, Zhao C Y, Wu X H and Ding S-J. 2022. Power-efficient gas-sensing and synaptic diodes based on lateral pentacene/a-IGZO PN junctions. *ACS Appl. Mater. Interfaces* **14**, 9368–9376.
- [88] Yang L, Wang Z X, Zhang S, Li Y, Jiang C P, Sun L and Xu W T. 2023. Neuromorphic gustatory system with salt-taste perception, information processing, and excessive-intake warning capabilities. *Nano Lett.* **23**, 8–16.
- [89] Liu J M, Qian J G, Adil M, Bi Y L, Wu H Y, Hu X F, Wang Z K and Zhang W. 2024. Bioinspired integrated triboelectric electronic tongue. *Microsyst. Nanoeng.* **10**, 57.
- [90] Jeong J-Y, Cha Y K, Ahn S R, Shin J, Choi Y, Park T H and Hong S. 2022. Ultrasensitive bioelectronic tongue based on the Venus flytrap domain of a human sweet taste receptor. *ACS Appl. Mater. Interfaces* **14**, 2478–2487.
- [91] Ghosh S, Pannone A, Sen D, Wali A, Ravichandran H and Das S. 2023. An all 2D bio-inspired gustatory circuit for mimicking physiology and psychology of feeding behavior. *Nat. Commun.* **14**, 6021.
- [92] Persaud K and Dodd G. 1982. Analysis of discrimination mechanisms in the mammalian olfactory system using a model nose. *Nature* **299**, 352–355.
- [93] Cho I et al. 2023. Deep-learning-based gas identification by time-variant illumination of a single micro-LED-embedded gas sensor. *Light Sci. Appl.* **12**, 95.
- [94] Wang C et al. 2024. Biomimetic olfactory chips based on large-scale monolithically integrated nanotube sensor arrays. *Nat. Electron.* **7**, 157–167.
- [95] Wang T, Huang H-M, Wang X-X and Guo X. 2021. An artificial olfactory inference system based on memristive devices. *InfoMat* **3**, 804–813.
- [96] Choudhry H H, Lee D H, Bag A and Lee N-E. 2023. A flexible artificial chemosensory neuronal synapse based on

- chemoreceptive ionogel-gated electrochemical transistor. *Nat. Commun.* **14**, 821.
- [97] Qian C, Choi Y, Choi Y J, Kim S, Choi Y Y, Roe D G, Kang M S, Sun J and Cho J H. 2020. Oxygen-detecting synaptic device for realization of artificial autonomic nervous system for maintaining oxygen homeostasis. *Adv. Mater.* **32**, 2002653.
- [98] Qian C, Choi Y, Kim S, Kim S, Choi Y J, Roe D G, Lee J H, Kang M S, Lee W H and Cho J H. 2022. Risk-perceptual and feedback-controlled response system based on NO₂-detecting artificial sensory synapse. *Adv. Funct. Mater.* **32**, 2112490.
- [99] Liu G C et al. 2022. Ultralow-power and multisensory artificial synapse based on electrolyte-gated vertical organic transistors. *Adv. Funct. Mater.* **32**, 2200959.
- [100] Han J-K, Park S-C, Yu J-M, Ahn J-H and Choi Y-K. 2022. A bioinspired artificial gustatory neuron for a neuromorphic based electronic tongue. *Nano Lett.* **22**, 5244–5251.
- [101] Pei Y F, Yan L, Wu Z H, Lu J K, Zhao J H, Chen J S, Liu Q and Yan X B. 2021. Artificial visual perception nervous system based on low-dimensional material photoelectric memristors. *ACS Nano* **15**, 17319–17326.
- [102] Wang H L et al. 2018. A ferroelectric/electrochemical modulated organic synapse for ultraflexible, artificial visual-perception system. *Adv. Mater.* **30**, 1803961.
- [103] Lee Y et al. 2018. Stretchable organic optoelectronic sensor-motor synapse. *Sci. Adv.* **4**, eaat7387.
- [104] Zhu S R, Xie T, Lv Z Y, Leng Y-B, Zhang Y-Q, Xu R Z, Qin J R, Zhou Y, Roy V A L and Han S-T. 2024. Hierarchies in visual pathway: functions and inspired artificial vision. *Adv. Mater.* **36**, 2301986.
- [105] Cho S W, Jo C, Kim Y-H and Park S K. 2022. Progress of materials and devices for neuromorphic vision sensors. *Nano-Micro Lett.* **14**, 203.
- [106] Wang R et al. 2022. Bio-inspired in-sensor compression and computing based on phototransistors. *Small* **18**, 2201111.
- [107] Zhou F C, Chen J W, Tao X M, Wang X R and Chai Y. 2019. 2D materials based optoelectronic memory: convergence of electronic memory and optical sensor. *Research* **2019**, 9490413.
- [108] Song J-K et al. 2022. Stretchable colour-sensitive quantum dot nanocomposites for shape-tunable multiplexed phototransistor arrays. *Nat. Nanotechnol.* **17**, 849–856.
- [109] Liao F Y et al. 2022. Bioinspired in-sensor visual adaptation for accurate perception. *Nat. Electron.* **5**, 84–91.
- [110] Islam M M et al. 2022. Multiwavelength optoelectronic synapse with 2D materials for mixed-color pattern recognition. *ACS Nano* **16**, 10188–10198.
- [111] Feng G D, Jiang J, Li Y R, Xie D D, Tian B B and Wan Q. 2021. Flexible vertical photogating transistor network with an ultrashort channel for in-sensor visual nociceptor. *Adv. Funct. Mater.* **31**, 2104327.
- [112] Zhou F C et al. 2019. Optoelectronic resistive random access memory for neuromorphic vision sensors. *Nat. Nanotechnol.* **14**, 776–782.
- [113] Kwon S M, Cho S W, Kim M, Heo J S, Kim Y-H and Park S K. 2019. Environment-adaptable artificial visual perception behaviors using a light-adjustable optoelectronic neuromorphic device array. *Adv. Mater.* **31**, 1906433.
- [114] Cui B Y et al. 2022. Ferroelectric photosensor network: an advanced hardware solution to real-time machine vision. *Nat. Commun.* **13**, 1707.
- [115] Cai Y C et al. 2023. Broadband visual adaption and image recognition in a monolithic neuromorphic machine vision system. *Adv. Funct. Mater.* **33**, 2212917.
- [116] Choi C et al. 2020. Curved neuromorphic image sensor array using a MoS₂-organic heterostructure inspired by the human visual recognition system. *Nat. Commun.* **11**, 5934.
- [117] He Z H, Shen H G, Ye D K, Xiang L Y, Zhao W R, Ding J M, Zhang F J, Di C-A and Zhu D B. 2021. An organic transistor with light intensity-dependent active photoadaptation. *Nat. Electron.* **4**, 522–529.
- [118] Hao Z Q et al. 2022. Retina-inspired self-powered artificial optoelectronic synapses with selective detection in organic asymmetric heterojunctions. *Adv. Sci.* **9**, 2103494.
- [119] Yang X Y, Xiong Z Y, Chen Y J, Ren Y, Zhou L, Li H L, Zhou Y, Pan F and Han S-T. 2020. A self-powered artificial retina perception system for image preprocessing based on photovoltaic devices and memristive arrays. *Nano Energy* **78**, 105246.
- [120] Gong Y, Xing X C, Lv Z Y, Chen J M, Xie P, Wang Y, Huang S M, Zhou Y and Han S-T. 2022. Ultrasensitive flexible memory phototransistor with detectivity of 1.8×10^{13} jones for artificial visual nociceptor. *Adv. Intell. Syst.* **4**, 2100257.
- [121] Meng J L, Wang T Y, Zhu H, Ji L, Bao W Z, Zhou P, Chen L, Sun Q-Q and Zhang D W. 2022. Integrated in-sensor computing optoelectronic device for environment-adaptable artificial retina perception application. *Nano Lett.* **22**, 81–89.
- [122] Pi L J et al. 2022. Broadband convolutional processing using band-alignment-tunable heterostructures. *Nat. Electron.* **5**, 248–254.
- [123] Zhao P F, Ji R X, Lao J, Jiang C L, Tian B B, Luo C H, Lin H C, Peng H and Duan C-G. 2022. Multifunctional two-terminal optoelectronic synapse based on zinc oxide/poly(3-hexylthiophene) heterojunction for neuromorphic computing. *ACS Appl. Polym. Mater.* **4**, 5688–5695.
- [124] Zhang J Y et al. 2023. Retina-inspired artificial synapses with ultraviolet to near-infrared broadband responses for energy-efficient neuromorphic visual systems. *Adv. Funct. Mater.* **33**, 2302885.
- [125] Shen C, Gao X, Chen C, Ren S, Xu J-L, Xia Y-D and Wang S-D. 2022. ZnO nanowire optoelectronic synapse for neuromorphic computing. *Nanotechnology* **33**, 065205.
- [126] Guo T, Zhang B Z, Wang X Y, Xiao Y, Sun B, Zhou Y N and Wu Y A. 2023. Broadband optoelectronic synapse enables compact monolithic neuromorphic machine vision for information processing. *Adv. Funct. Mater.* **33**, 2303879.
- [127] Kim J, Song S, Lee J-M, Nam S, Kim J, Hwang D K, Park S K and Kim Y-H. 2023. Metal-oxide heterojunction optoelectronic synapse and multilevel memory devices enabled by broad spectral photocarrier modulation. *Small* **19**, 2301186.
- [128] Kwon S M et al. 2021. Large-area pixelized optoelectronic neuromorphic devices with multispectral light-modulated bidirectional synaptic circuits. *Adv. Mater.* **33**, 2105017.
- [129] Lao J et al. 2022. Ultralow-power machine vision with self-powered sensor reservoir. *Adv. Sci.* **9**, 2106092.
- [130] Guo L Q, Sun H X, Min L L, Wang M, Cao F R and Li L. 2024. Two-terminal perovskite optoelectronic synapse for rapid trained neuromorphic computation with high accuracy. *Adv. Mater.* **36**, 2402253.
- [131] Gao Z X, Ju X, Zhang H Z, Liu X H, Chen H Y, Li W F, Zhang H L, Liang L Y and Cao H T. 2023. InP quantum dots tailored oxide thin film phototransistor for bioinspired visual adaptation. *Adv. Funct. Mater.* **33**, 2305959.
- [132] Liang K et al. 2022. Fully printed optoelectronic synaptic transistors based on quantum dot-metal oxide semiconductor heterojunctions. *ACS Nano* **16**, 8651–8661.
- [133] Zhou G D et al. 2023. Full hardware implementation of neuromorphic visual system based on multimodal optoelectronic resistive memory arrays for versatile image processing. *Nat. Commun.* **14**, 8489.

- [134] Zhu X T, Gao C S, Ren Y W, Zhang X H, Li E L, Wang C Y, Yang F X, Wu J S, Hu W P and Chen H P. 2023. High-contrast bidirectional optoelectronic synapses based on 2D molecular crystal heterojunctions for motion detection. *Adv. Mater.* **35**, 2301468.
- [135] Wu X S, Shi S H, Liang B S, Dong Y, Yang R M, Ji R D, Wang Z R and Huang W G. 2024. Ultralow-power optoelectronic synaptic transistors based on polyzwitterion dielectrics for in-sensor reservoir computing. *Sci. Adv.* **10**, eadn4524.
- [136] Chaves A et al. 2020. Bandgap engineering of two-dimensional semiconductor materials. *npj 2D Mater. Appl.* **4**, 29.
- [137] Chen T, Gao X, Zhang J-Y, Xu J-L and Wang S-D. 2020. Ultrasensitive ZnO nanowire photodetectors with a polymer electret interlayer for minimizing dark current. *Adv. Opt. Mater.* **8**, 1901289.
- [138] Zhang Z H, Wang S Y, Liu C S, Xie R Z, Hu W D and Zhou P. 2022. All-in-one two-dimensional retinomorphic hardware device for motion detection and recognition. *Nat. Nanotechnol.* **17**, 27–32.
- [139] Sangwan V K and Hersam M C. 2020. Neuromorphic nanoelectronic materials. *Nat. Nanotechnol.* **15**, 517–528.
- [140] Xu K M, Zhou W J and Ning Z J. 2020. Integrated structure and device engineering for high performance and scalable quantum dot infrared photodetectors. *Small* **16**, 2003397.
- [141] Zhao Y S, Fu H B, Peng A D, Ma Y, Liao Q and Yao J N. 2010. Construction and optoelectronic properties of organic one-dimensional nanostructures. *Acc. Chem. Res.* **43**, 409–418.
- [142] Lee Y, Min S-Y, Kim T-S, Jeong S-H, Won J Y, Kim H, Xu W T, Jeong J K and Lee T-W. 2016. Versatile metal nanowiring platform for large-scale nano- and optoelectronic devices. *Adv. Mater.* **28**, 9109–9116.
- [143] He Z, Yang Y, Liang H-W, Liu J-W and Yu S-H. 2019. Nanowire genome: a magic toolbox for 1D nanostructures. *Adv. Mater.* **31**, 1902807.
- [144] Mak K F and Shan J. 2016. Photonics and optoelectronics of 2D semiconductor transition metal dichalcogenides. *Nat. Photon.* **10**, 216–226.
- [145] Novoselov K S, Mishchenko A, Carvalho A and Castro Neto A H. 2016. 2D materials and van der Waals heterostructures. *Science* **353**, aac9439.
- [146] Ma S L et al. 2022. A 619-pixel machine vision enhancement chip based on two-dimensional semiconductors. *Sci. Adv.* **8**, eabn9328.
- [147] Lopez-Sanchez O, Lembke D, Kayci M, Radenovic A and Kis A. 2013. Ultrasensitive photodetectors based on monolayer MoS₂. *Nat. Nanotechnol.* **8**, 497–501.
- [148] Qiao J S, Kong X H, Hu Z-X, Yang F and Ji W. 2014. High-mobility transport anisotropy and linear dichroism in few-layer black phosphorus. *Nat. Commun.* **5**, 4475.
- [149] Hong T, Chamlagain B, Wang T J, Chuang H-J, Zhou Z X and Xu Y-Q. 2015. Anisotropic photocurrent response at black phosphorus–MoS₂ p–n heterojunctions. *Nanoscale* **7**, 18537–18541.
- [150] Li L K, Yu Y J, Ye G J, Ge Q Q, Ou X D, Wu H, Feng D L, Chen X H and Zhang Y B. 2014. Black phosphorus field-effect transistors. *Nat. Nanotechnol.* **9**, 372–377.
- [151] Liu H W, Hu K, Yan D F, Chen R, Zou Y Q, Liu H B and Wang S Y. 2018. Recent advances on black phosphorus for energy storage, catalysis, and sensor applications. *Adv. Mater.* **30**, 1800295.
- [152] Lee S, Peng R M, Wu C M and Li M. 2022. Programmable black phosphorus image sensor for broadband optoelectronic edge computing. *Nat. Commun.* **13**, 1485.
- [153] Setter N et al. 2006. Ferroelectric thin films: review of materials, properties, and applications. *J. Appl. Phys.* **100**, 051606.
- [154] Zhou X Y, Ke Q Q, Tang S L, Luo J L and Lu Z H. 2023. Ultraviolet photodetectors based on ferroelectric depolarization field. *J. Energy Chem.* **77**, 487–498.
- [155] Root S E, Savagatrup S, Printz A D, Rodriguez D and Lipomi D J. 2017. Mechanical properties of organic semiconductors for stretchable, highly flexible, and mechanically robust electronics. *Chem. Rev.* **117**, 6467–6499.
- [156] Søndergaard R R, Hösel M and Krebs F C. 2013. Roll-to-roll fabrication of large area functional organic materials. *J. Polym. Sci. B* **51**, 16–34.
- [157] Lee Y R, Trung T Q, Hwang B-U and Lee N-E. 2020. A flexible artificial intrinsic-synaptic tactile sensory organ. *Nat. Commun.* **11**, 2753.
- [158] Yang B et al. 2020. Bioinspired multifunctional organic transistors based on natural chlorophyll/organic semiconductors. *Adv. Mater.* **32**, 2001227.
- [159] Deng W, Zhang X J, Jia R F, Huang L M, Zhang X H and Jie J S. 2019. Organic molecular crystal-based photosynaptic devices for an artificial visual-perception system. *NPG Asia Mater.* **11**, 77.
- [160] Baek E et al. 2020. Intrinsic plasticity of silicon nanowire neurotransistors for dynamic memory and learning functions. *Nat. Electron.* **3**, 398–408.
- [161] Ji D Y et al. 2019. Band-like transport in small-molecule thin films toward high mobility and ultrahigh detectivity phototransistor arrays. *Nat. Commun.* **10**, 12.
- [162] Liu J Y, Zhou K, Liu J, Zhu J, Zhen Y G, Dong H L and Hu W P. 2018. Organic-single-crystal vertical field-effect transistors and phototransistors. *Adv. Mater.* **30**, 1803655.
- [163] Shen H G, He Z H, Jin W L, Xiang L Y, Zhao W R, Di C-A and Zhu D B. 2019. Mimicking sensory adaptation with dielectric engineered organic transistors. *Adv. Mater.* **31**, 1905018.
- [164] Han T-H, Tan S, Xue J J, Meng L, Lee J-W and Yang Y. 2019. Interface and defect engineering for metal halide perovskite optoelectronic devices. *Adv. Mater.* **31**, 1803515.
- [165] Jin C X et al. 2022. Artificial vision adaption mimicked by an optoelectrical In₂O₃ transistor array. *Nano Lett.* **22**, 3372–3379.
- [166] Lee T-J, Yun K-R, Kim S-K, Kim J-H, Jin J, Sim K-B, Lee D-H, Hwang G W and Seong T-Y. 2021. Realization of an artificial visual nervous system using an integrated optoelectronic device array. *Adv. Mater.* **33**, 2105485.
- [167] Shan X Y et al. 2022. Plasmonic optoelectronic memristor enabling fully light-modulated synaptic plasticity for neuromorphic vision. *Adv. Sci.* **9**, 2104632.
- [168] Dodda A et al. 2022. Active pixel sensor matrix based on monolayer MoS₂ phototransistor array. *Nat. Mater.* **21**, 1379–1387.
- [169] Demb J B. 2008. Functional circuitry of visual adaptation in the retina. *J. Physiol.* **586**, 4377–4384.
- [170] Mante V, Frazor R A, Bonin V, Geisler W S and Carandini M. 2005. Independence of luminance and contrast in natural scenes and in the early visual system. *Nat. Neurosci.* **8**, 1690–1697.
- [171] Gonzalezharo C, Gonzalezdesuso J, Padullés J, Drobnic F and Escanero J. 2005. Physiological adaptation during short distance triathlon swimming and cycling sectors simulation. *Physiol. Behav.* **86**, 467–474.
- [172] Hong S, Choi S H, Park J, Yoo H, Oh J Y, Hwang E, Yoon D H and Kim S. 2020. Sensory adaptation and neuromorphic phototransistors based on CsPb(Br_{1-x}I_x)₃ perovskite and MoS₂ hybrid structure. *ACS Nano* **14**, 9796–9806.
- [173] Liu W Z, Yang X H, Wang Z Q, Li Y Z, Li J X, Feng Q S, Xie X H, Xin W, Xu H Y and Liu Y C. 2023. Self-powered and broadband opto-sensor with bionic visual adaptation function based on multilayer γ -InSe flakes. *Light Sci. Appl.* **12**, 180.

- [174] Xie D D, Gao G, Tian B B, Shu Z W, Duan H G, Zhao W-W, He J and Jiang J. 2023. Porous metal-organic framework/ReS₂ heterojunction phototransistor for polarization-sensitive visual adaptation emulation. *Adv. Mater.* **35**, 2212118.
- [175] Wen W et al. 2024. Biomimetic nanocluster photoreceptors for adaptive circular polarization vision. *Nat. Commun.* **15**, 2397.
- [176] Wang C-Y et al. 2020. Gate-tunable van der Waals heterostructure for reconfigurable neural network vision sensor. *Sci. Adv.* **6**, eaba6173.
- [177] Wang Y et al. 2024. Monolithic 2D perovskites enabled artificial photonic synapses for neuromorphic vision sensors. *Adv. Mater.* **36**, 2311524.
- [178] Fu X et al. 2023. Graphene/MoS_{2-x}O_x/graphene photomemristor with tunable non-volatile responsivities for neuromorphic vision processing. *Light Sci. Appl.* **12**, 39.
- [179] Mennel L, Symonowicz J, Wachter S, Polyushkin D K, Molina-Mendoza A J and Mueller T. 2020. Ultrafast machine vision with 2D material neural network image sensors. *Nature* **579**, 62–66.
- [180] Wang X, Lu Y, Zhang J Y, Zhang S Q, Chen T Q, Ou Q Q and Huang J. 2021. Highly sensitive artificial visual array using transistors based on porphyrins and semiconductors. *Small* **17**, 2005491.
- [181] Sun L, Qu S D, Du Y, Yang L, Li Y, Wang Z X and Xu W T. 2023. Bio-inspired vision and neuromorphic image processing using printable metal oxide photonic synapses. *ACS Photonics* **10**, 242–252.
- [182] Leydecker T, Herder M, Pavlica E, Bratina G, Hecht S, Orgiu E and Samorì P. 2016. Flexible non-volatile optical memory thin-film transistor device with over 256 distinct levels based on an organic bicomponent blend. *Nat. Nanotechnol.* **11**, 769–775.
- [183] Xue F et al. 2020. Optoelectronic ferroelectric domain-wall memories made from a single van der Waals ferroelectric. *Adv. Funct. Mater.* **30**, 2004206.
- [184] Lee D, Yang S M, Kim T H, Jeon B C, Kim Y S, Yoon J-G, Lee H N, Baek S H, Eom C B and Noh T W. 2012. Multilevel data storage memory using deterministic polarization control. *Adv. Mater.* **24**, 402–406.
- [185] Zhang J R, Zhang J, Lok T M and Lyu M R. 2007. A hybrid particle swarm optimization-back-propagation algorithm for feedforward neural network training. *Appl. Math. Comput.* **185**, 1026–1037.
- [186] Quraishi I, Choudhury J P and De M. 2012. Image recognition and processing using Artificial Neural Network. *In Proceedings 2012 1st International Conference on Recent Advances in Information Technology (IEEE)* pp 95–100
- [187] Yu J R, Yang X XX, Gao G, Xiong Y F, Wang Y, Han J, Chen Y, Zhang H, Sun Q and Wang Z L. 2021. Bioinspired mechano-photonic artificial synapse based on graphene/MoS₂ heterostructure. *Sci. Adv.* **7**, eabd9117.
- [188] Gu L J, Li Y R, Xie D D and Jiang J. 2022. Fully optical-driving ionotronic InGaZnO₄ phototransistor for gate-tunable bidirectional photofiltering and visual perception. *IEEE Trans. Electron Devices* **69**, 4382–4385.
- [189] Gu J X et al. 2018. Recent advances in convolutional neural networks. *Pattern Recognit.* **77**, 354–377.
- [190] Wang S et al. 2021. Networking retinomorphic sensor with memristive crossbar for brain-inspired visual perception. *Natl Sci. Rev.* **8**, nwaal72.
- [191] Jo C, Kim J, Kwak J Y, Kwon S M, Park J B, Kim J, Park G-S, Kim M-G, Kim Y-H and Park S K. 2022. Retina-inspired color-cognitive learning via chromatically controllable mixed quantum dot synaptic transistor arrays. *Adv. Mater.* **34**, 2108979.
- [192] Lukoševičius M and Jaeger H. 2009. Reservoir computing approaches to recurrent neural network training. *Comput. Sci. Rev.* **3**, 127–149.
- [193] Tanaka G, Yamane T, Héroux J B, Nakane R, Kanazawa N, Takeda S, Numata H, Nakano D and Hirose A. 2019. Recent advances in physical reservoir computing: a review. *Neural Netw.* **115**, 100–123.
- [194] Chen Y X, Fang F Z and Zhang N. 2024. Advance in additive manufacturing of 2D materials at the atomic and close-to-atomic scale. *npj 2D Mater. Appl.* **8**, 17.
- [195] Serra P and Piqué A. 2019. Laser-induced forward transfer: fundamentals and applications. *Adv. Mater. Technol.* **4**, 1800099.
- [196] Xu H C et al. 2023. A fully integrated, standalone stretchable device platform with in-sensor adaptive machine learning for rehabilitation. *Nat. Commun.* **14**, 7769.
- [197] Bello H O, Ige A B and Ameyaw M N. 2024. Adaptive machine learning models: concepts for real-time financial fraud prevention in dynamic environments. *World J. Adv. Eng. Technol. Sci.* **12**, 21–34.
- [198] Gligorea I, Cioca M, Oancea R, Gorski A-T, Gorski H and Tudorache P. 2023. Adaptive learning using artificial intelligence in e-learning: a literature review. *Educ. Sci.* **13**, 1216.
- [199] Akintuyi O B. 2024. Adaptive AI in precision agriculture: a review: investigating the use of self-learning algorithms in optimizing farm operations based on real-time data. *J. Multidiscip. Stud.* **7**, 16–30.
- [200] Rashid K, Saeed Y, Ali A, Jamil F, Alkanhel R and Muthanna A. 2023. An adaptive real-time malicious node detection framework using machine learning in vehicular Ad-Hoc networks (VANETs). *Sensors* **23**, 2594.
- [201] Wu L, Huang X D, Cui J G, Liu C and Xiao W S. 2023. Modified adaptive ant colony optimization algorithm and its application for solving path planning of mobile robot. *Expert Syst. Appl.* **215**, 119410.
- [202] Song T B, Hu W J, Cai J F, Liu W J, Yuan Q and He K. 2023. Bio-inspired swarm intelligence: a flocking project with group object recognition. *In Proceedings 2023 3rd International Conference on Consumer Electronics and Computer Engineering (IEEE)* pp 834–837
- [203] Li L H, Liu L L, Shao Y X, Zhang X, Chen Y, Guo C and Nian H. 2023. Enhancing swarm intelligence for obstacle avoidance with multi-strategy and improved dung beetle optimization algorithm in mobile robot navigation. *Electronics* **12**, 4462.